Australian Government
Department of Defence
Defence Science and
Technology Organisation

Experimental Plan for the Development of Equivalent Crack Size Distributions and a Monte Carlo Model of Fatigue in Low and High-k_t Specimens of Corroded AA7050-T7451

Bruce R. Crawford, Timothy J. Harrison, Chris Loader and P. Khan Sharp

Air Vehicles Division
Defence Science and Technology Organisation

DSTO-TN-1073

ABSTRACT

Fatigue life data from low and high-k_t specimen are difficult to compare due to the smaller sampling volume of high-k_t specimens. As a result, equivalent crack size (ECS) distributions developed using low-k_t specimens cannot be used in high-k_t conditions such as near fastener holes. This experimental plan addresses this issue for corroded AA7050-T7451. Fatigue crack growth (FCG) and fatigue life tests will be conducted on low and high-k_t specimens which have been designed to minimise the differences between the specimens other than the different stress field. FCG data and ECS distributions will be developed for both specimens types. A Monte Carlo model will then be used to test if the low-k_t ECS distribution can accurately predict the fatigue lives of the high-k_t specimens. If successful, this will allow low-k_t ECS distributions, which are easier to derive, to be used under high-k_t conditions.

RELEASE LIMITATION

Approved for public release

Published by

Air Vehicles Division
DSTO Defence Science and Technology Organisation
506 Lorimer St
Fishermans Bend, Victoria 3207 Australia

Telephone: (03) 9626 7000
Fax: (03) 9626 7999

AR-015-242
March 2012

APPROVED FOR PUBLIC RELEASE

Experimental Plan for the Development of Equivalent Crack Size Distributions and a Monte Carlo Model of Fatigue in Low and High-k_t Specimens of Corroded AA7050-T7451

Executive Summary

Corrosion of the fastener holes in modern aircraft, such as the fleet of the Australian Defence Force is a widespread and persistent problem. It is desirable to be able to accurately predict how this corrosion affects the fatigue performance of aircraft. However, it is difficult to compare fatigue life data from low and high-k_t specimens due to the greatly reduced sampling volume of high-k_t fatigue specimens. This means that equivalent crack size (ECS) distributions for corroded material developed using low-k_t specimens are typically of limited use in high-k_t conditions such as near a fastener hole in an airframe. This is problematic as ECS distributions are easier to develop under low-k_t test conditions.

The experimental plan addresses this issue. Fatigue crack growth and fatigue life tests will be conducted on low and high-k_t specimens of corroded AA7050-T7451. These specimens have been designed to minimise the differences between the specimens other than the difference in stress field. Fatigue crack growth data and equivalent crack size distributions will be developed from both the low and high-k_t specimens. A Monte Carlo simulation will then be used to see if the ECS distribution from the low-k_t specimens can accurately predict the fatigue lives of the high-k_t specimens. If this approach is successful, it will be possible to use low-k_t equivalent crack size distributions, which are easier to derive, to predict the fatigue behaviour under high-k_t conditions.

This page is intentionally blank

Contents

Glossary

AFGROW	Air Force Grow, a fatigue crack growth prediction software package
AFRL	(United States Air Force) Air Force Research Laboratory
A_{hole}	Area of the bore of the hole in the high-k_t specimens
ASTM	American Society for Testing and Materials
AVD	Air Vehicles Division of DSTO
CSIRO	Commonwealth Scientific and Industrial Research Organisation
da/dN	Fatigue crack growth rate (mm/cycle)
DDP	Design Development Plan
DGTA	Directorate General Technical Airworthiness
DSTO	Defence Science and Technology Organisation
ECS	Equivalent Crack Size (methodology)
FCG	Fatigue Crack Growth
ID	Identification
k_t	Elastic Stress Concentration Factor
$k_{t,high}$	k_t value of high-k_t fatigue specimens
$k_{t,low}$	k_t value of low-k_t fatigue specimens
L	Longitudinal (i.e. rolling) direction in plate
LRR	Long Range Research
MX	Identification of AA7050-T7451 plate used in this work
NASA	(US) National Aeronautical and Space Administration
NATA	(Australian) National Association of Testing Authorities
N_f	Cycles to failure or Fatigue Life
pH	Measure of acidity in aqueous solutions
R	Load Ratio = $\sigma_{min}/\sigma_{max}$
RAAF	Royal Australian Air Force
S	Short-transverse direction in plate
SEM	Scanning Electron Microscope
SICAS	Structural Integrity effects of Corrosion in Aircraft Structures
SOR	Statement of Requirement
T	Long-transverse direction in plate
TAMM	Technical Airworthiness Management Manual
TFSPO	Tactical Fighter Systems Program Office
TRL	Technological Reading Level
USAF	United States Air Force
ΔK	Cyclic Stress Intensity Factor Range (MPa$\sqrt{m}$)
$\sigma_{applied}$	Applied Stress (MPa)
σ_{max}	Maximum Stress (MPa)
σ_{min}	Minimum Stress (MPa)

This page is intentionally blank

1. Introduction

This technical note outlines the experimental plan for testing and analysis of the fatigue specimens machined from the plate of AA7050-T7451 designated MX in the project '*The Effect of Pitting and Intergranular Corrosion on the Structural Integrity of 7050-T7451*'. This project is part of the Air Vehicles Division's enabling research program under Task LRR 07/250. The aim of this project is to develop the Equivalent Crack Size (ECS) methodology to a technological readiness level (TRL) of five from its current TRL of two or three, and to facilitate the subsequent development of this technology by a partnership between the Defence Science and Technology Organisation (DSTO), the Directorate General of Technical Airworthiness (DGTA) and the Tactical Fighter Systems Program Office (TFSPO).

Given the intent to transfer the ECS methodology into service on Royal Australian Air Force (RAAF) aircraft, it is necessary to conform with the certification requirements of the RAAF's Technical Airworthiness Management Manual (TAMM) [1]. The TAMM requires that any design must have a Statement of Requirement (SOR) and a Design Development Plan (DDP) prior to work starting. In the absence of a SOR from TFSPO, the Corrosion Structural Integrity Roadmap [2] is the SOR for this work while this current report can be considered to be the DDP.

2. Previous Work

This section briefly summarises the results from previous DSTO work in this area to facilitate the design of the experimental matrix in the current project. Results from Crawford and Sharp [3], Crawford et al. [4, 5] and Crawford et al. [6] are examined in this section. A more detailed summary of the first two of these datasets may be found in [2]. The purpose of this section is to assist with the selection of the cyclic and maximum stresses for the experimental matrix described in Section 3.3.6.

2.1 AA7050-T7451 High-k_t End Grain Project (F/A-18)

This section examines the results obtained by Sharp during a long-term attachment at the United States Air Force Research Laboratory (USAF-AFRL) in Ohio, USA in 1999 [7]. During this attachment, Sharp conducted fatigue life tests on corroded and uncorroded high-k_t specimens of AA7050-T7451. It can be seen in Figure 1 that corrosion has reduced the fatigue life of the AA7050-T7451 material. Table 1 summaries the experimental matrix used by Sharp. It shows the applied stress, $\sigma_{applied}$, which was calculated by dividing the applied load by the cross-sectional area of the specimen's gauge section (neglecting the cross-sectional area of the hole) and the maximum stress, σ_{max}, which is the applied stress multiplied by the calculated stress concentration factor of 3.15. Two of the five maximum stress levels are above the A-basis yield stress of the material (60 ksi = 414 MPa) [7]. These are indicated by red bold figures in Table 1.

This table also gives the log-average[1] cycles to failure of the corroded and uncorroded specimens at each of the five stress levels tested. The results are as expected with the corroded material having a shorter fatigue life than the uncorroded material at all stress levels tested.

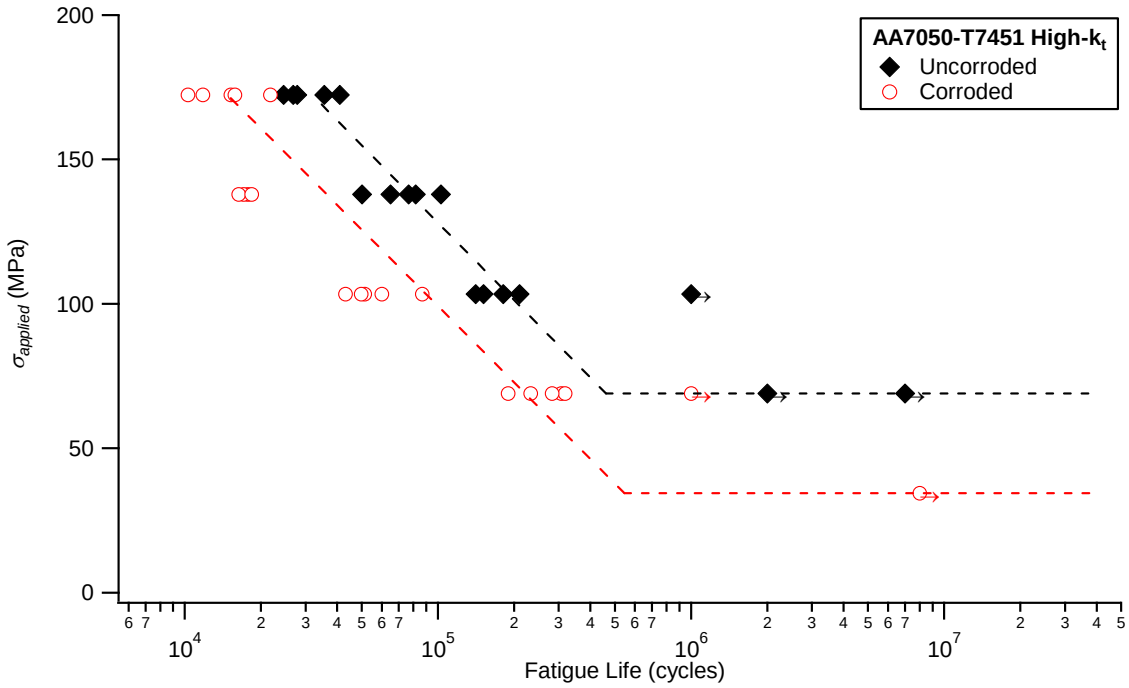

Figure 1: Comparison of fatigue lives of as-machined and corroded AA7050-T7451 high-k_t versus $\sigma_{applied}$. All tests were conducted at R = 0.1. Arrows on data points indicate runouts.

Table 1: Log-average fatigue life results for as-machined finish and corroded finish versus stress. σ_{max} values in bold and red exceed the A-basis 60 ksi (414 MPa) yield stress value of six-inch AA7050-T7451 plate published in MMPDS-01 [7].

$\sigma_{applied}$ (MPa)	σ_{max} (MPa)*	As-Machined S (log-average cycles)	Corroded Specimens (log-average cycles)
34	108	N/A	$> 5 \times 10^6$
69	219	$> 5 \times 10^6$	261×10^3
103	328	169×10^3	56.5×10^3
138	**439**	73.2×10^3	17.4×10^3
172	**547**	30.6×10^3	14.5×10^3

* To determine actual stress at the edge of the hole, multiply the $\sigma_{applied}$ by 3.15

[1] Log-average fatigue life = $10^{\frac{1}{n}\sum_{i=1}^{n}\log_{10}(N_{f,i})}$, where $N_{f,i}$ is the fatigue life of the i-th specimen (i.e. its cycles to failure) and n is the total number of specimens tested

2.2 AA7010-T7651 Low-k_t Surface Grain (Hawk)

Following the work by Sharp discussed in the previous section DSTO [3], studied the effect of pitting corrosion on the fatigue endurance of AA7010-T7651 in collaboration with CSIRO and BAE SYSTEMS [4, 5]. This was the so-called SICAS[2] project. The fatigue life results from this study are shown in Figure 2. Table 2 gives the log-average fatigue lives at each of the twelve load conditions tested.

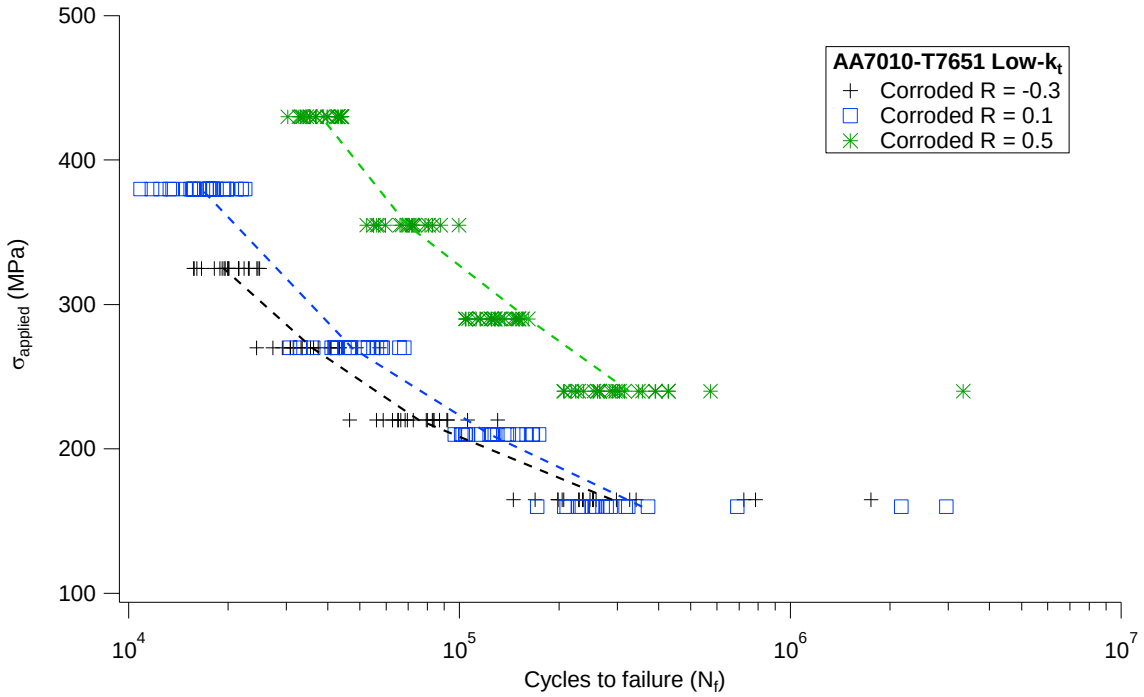

Figure 2: Results of constant amplitude fatigue life tests showing effect of stress and load ratio on fatigue life on corroded AA7010-T7651 versus $\sigma_{applied}$

Table 2: Log-average fatigue life results for corroded AA7010-T7651 low-k_t specimens vs. $\sigma_{applied}$

Stress Level	*R* = -0.3		*R* = 0.1		*R* = 0.5	
	$\sigma_{applied}$ (MPa)	Log-average fatigue life	$\sigma_{applied}$ (MPa)	Log-average fatigue life	$\sigma_{applied}$ (MPa)	Log-average fatigue life
Low	165	289×10^3	160	357×10^3	240	326×10^3
Mid-Low	220	75.4×10^3	210	123×10^3	290	161×10^3
Mid-High	270	35.9×10^3	270	47.3×10^3	335	69.7×10^3
High	325	19.4×10^3	380	16.6×10^3	430	38.2×10^3

[2] SICAS = Structural Integrity effects of Corrosion in Aircraft Structures

2.3 AA7050-T7451 Low-k_t Surface Grain and End Grain ECS Model

In 2007 and 2008, a series of fatigue life tests were conducted on low-k_t specimens of the same design as those from the SICAS project machined from AA7050-T7451. These specimens were machined in two orientations (L-T and L-S) which are shown in Figure 3 below. The results of the tests on the surface grain corroded specimens are shown in Figure 4 versus the applied stress, $\sigma_{applied}$. These results have not previously been published. Table 3 summarises the fatigue lives of the surface corroded specimens for each load condition tested as a log-average. The end-grain specimens for this work were machined but have not yet been corroded and tested.

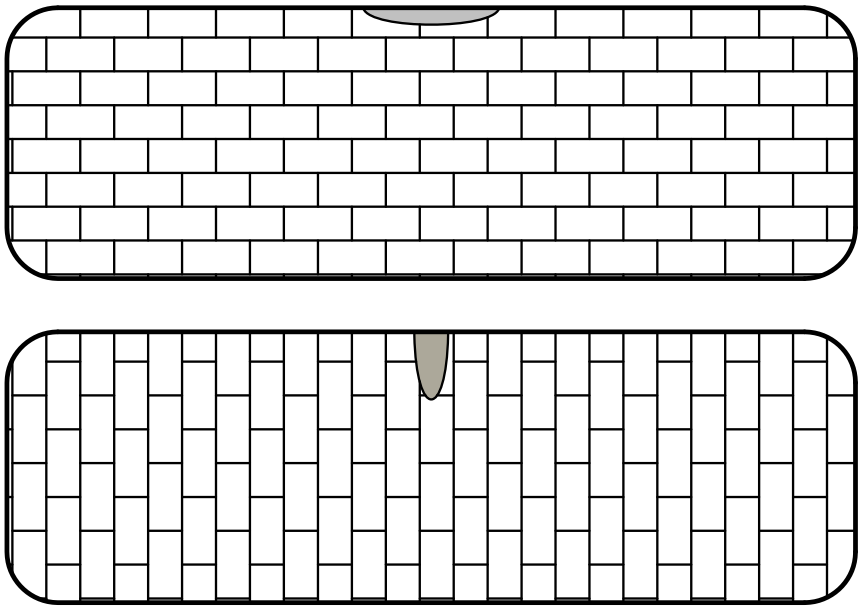

Figure 3: Orientation of microstructure and corrosion pitting relative to the cross-section of the specimens used in the (a) surface and (b) end-grain fatigue specimens. The rectangles inside the cross-sections represent the orientation of the grain structures in each specimen. The size of these grains, however, has been greatly enlarged for clarity.

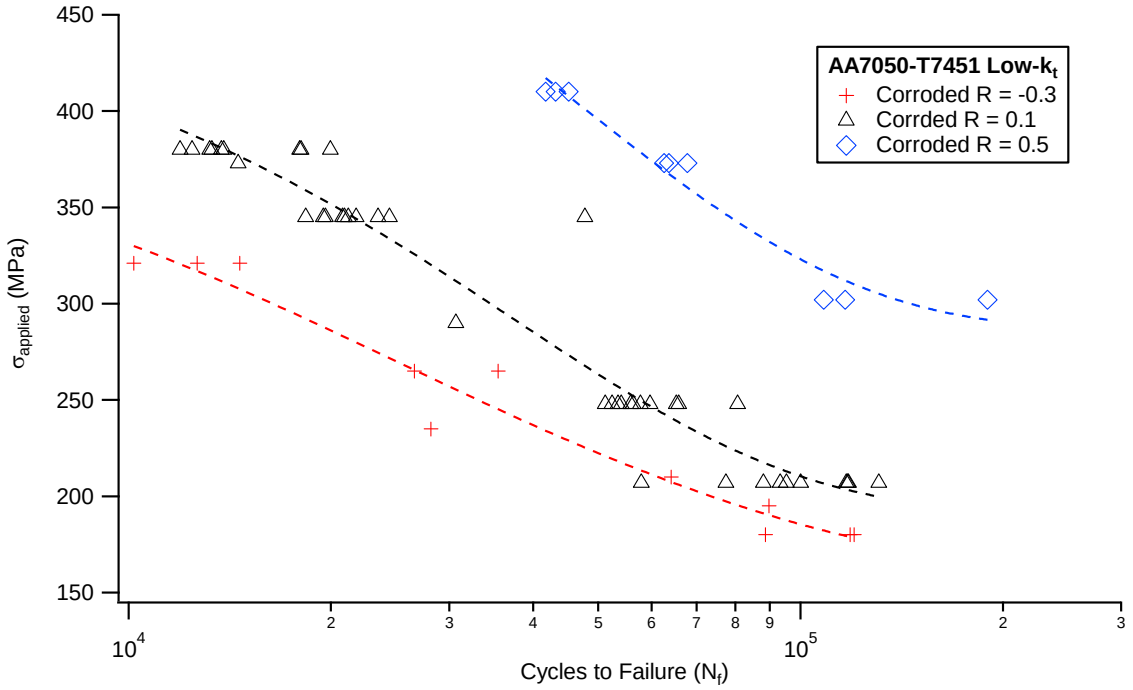

Figure 4: Results of constant amplitude fatigue life tests showing effect of stress and load ratio on fatigue life in surface grain corroded AA7050-T4651 as a function of $\sigma_{applied}$

Table 3: Log-average fatigue life results corroded for corroded AA7050-T7451 low-k_t specimens versus $\sigma_{applied}$

Stress Level	***R* = -0.3**		***R* = 0.1**		***R* = 0.5**	
	$\sigma_{applied}$ (MPa)	**Log-average fatigue life**	**$\sigma_{applied}$ (MPa)**	**Log-average fatigue life**	**$\sigma_{applied}$ (MPa)**	**Log-average fatigue life**
Low	180	108×10^3	207	97.1×10^3	302	134×10^3
Mid-Low	265	30.7×10^3	248	58.8×10^3	373	64.7×10^3
Mid-High	321	12.4×10^3	345	22.9×10^3	410	43.3×10^3
High	–	–	380	14.7×10^3	–	–

2.4 Comparison of Results of Previous Work

Figure 5 and Figure 6 compare the R = 0.1 fatigue life data from each of the previous three sections. In these graphs fatigue lives are plotted against σ_{max}, the maximum stress, rather than $\sigma_{applied}$, the applied stress. σ_{max} was calculated using the standard formula, which is [8]:

$$\sigma_{max} = k_t \times \sigma_{applied} \quad (1)$$

where k_t = 1.04 for the low-k_t specimens, and
= 3.15 for the high-k_t specimens (see Section 3.3.6.1).

From examination of Figure 5 and Figure 6 it appears that the fatigue life results from all three data sources are similar when plotted as a function of the maximum stress, σ_{max}, calculated using Equation (1). This is especially true of the two sets of low-k_t fatigue life results for AA7050-T7451 and AA7010-T7651. The high-k_t results for AA7050-T7451 have log-average lives that are about 70% longer than the log-average lives of the low-k_t specimens at the same σ_{max}. It is hypothesised that the longer lives of the high-k_t specimens are at least partly due to the reduced sampling volume created by the stress concentrator in these specimens. This provides some support the hypothesis of this experimental plan that an ECS distribution calculated from low-k_t fatigue life results can be used in a high-k_t loading situation. However, it should be noted that the pit size distributions in each of the three cases were different. This is one of the deficiencies that this experimental plan was developed to address.

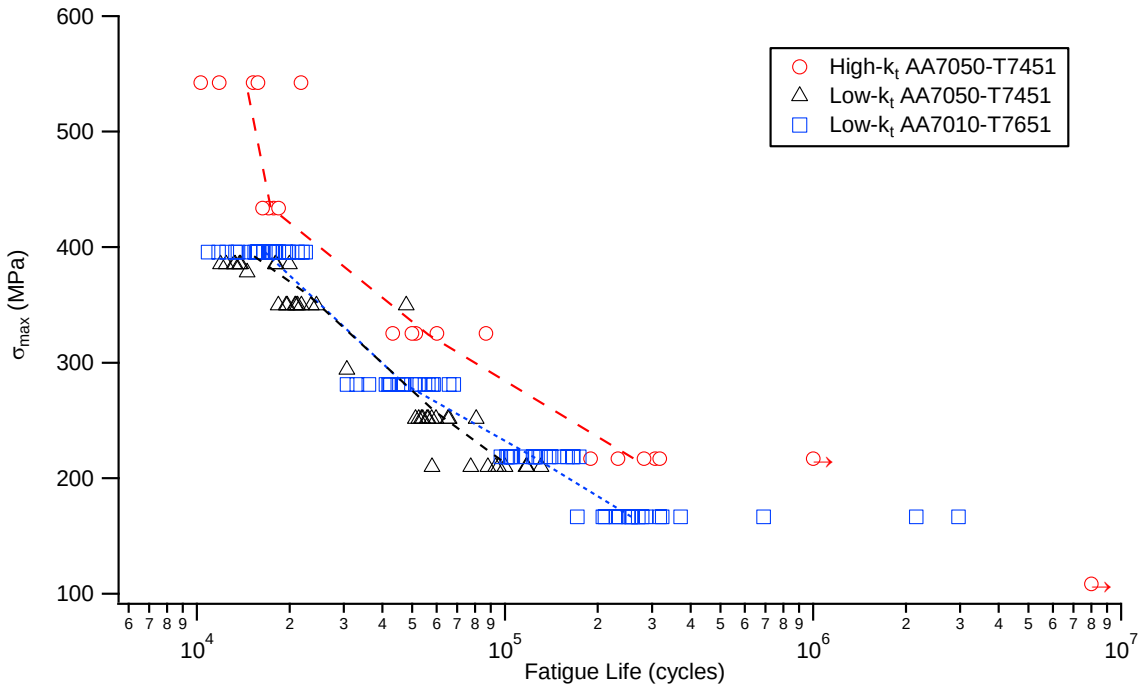

Figure 5: Comparison of all fatigue life results from Sharp and Crawford [3], Crawford et al. [4, 5] and Section 2.3 at R = 0.1

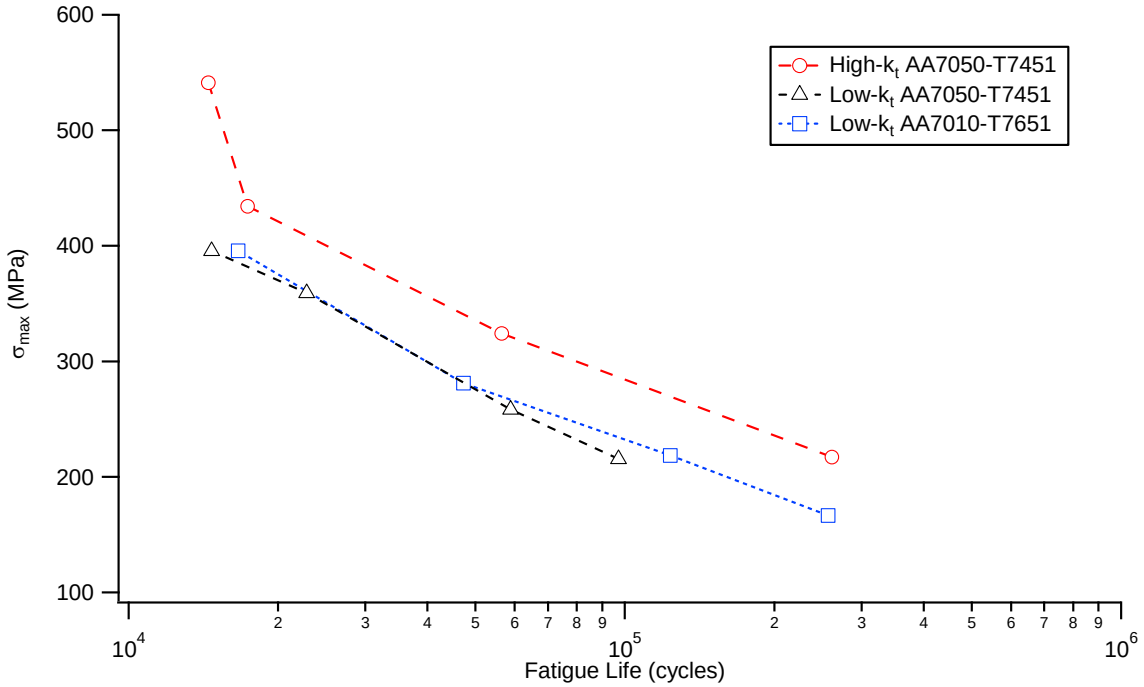

Figure 6: Comparison of log-average fatigue life results from Sharp and Crawford [3], Crawford et al. [4, 5] and Section 2.3 at R = 0.1

3. Experimental Details

3.1 Aim

The aim of the experimental plan described in this technical note is to study the effect of different local stress fields on the application of the ECS methodology. This will allow results collected from corroded low-k_t specimens to be used in high-k_t loading situations where corrosion is present, such as near a corroded fastener hole.

The above aim will be achieved by fatigue testing low-k_t and high-k_t fatigue specimens of 7075-T7451 under conditions that are as close to identical as possible. The low and high-k_t specimens will be orientated so that the material's end-grain is exposed to the corrosive environment in each case. The specimens will then be fatigue tested at constant amplitude using equal local maximum stress values. The fatigue cracks will be growing in the same plane in both specimen types.

3.2 Material

The material to be used in this experimental program is a six inch thick rolled plate of the aluminium alloy AA7050-T7451. This alloy is the primary structural alloy in the F/A-18 Hornet, the F/A-18E-F Super Hornet and the F-35 Lightning II. The first two of these aircraft

are currently in RAAF service and the third is expected to enter RAAF service in the near future.

The rolled plate for this work was purchased from Thyssen Krupp Aerospace Australia on the 23 September 2011[3]. According to its inspection certificate (Appendix A) it is 152.4 mm thick, 1,220 mm wide x 3,660 mm long. It was entered into the AVD Materials Register, along with a scanned PDF of its inspection certificate on the 20th of October 2011 [9].

3.3 Experimental Plan

The experimental programme for this work will consist of eight stages. These are:

1. **Bulk Cut-Up of MX Plate:** The AA7050-T7451 rolled plate will be cut-up to produce specimens for low and high-k_t fatigue testing, microstructural characterisation and corrosion protocol development. Specimens for corrosion testing and microstructural characterisation will also be machined during this stage.
2. **Microstructural Characterisation:** In this stage the microstructure of the experimental material will be characterised to determine the size distribution of the constituent particles in it matrix and the size distribution of its grains.
3. **Corrosion Protocol Development:** The corrosion protocol used in Crawford and Sharp [3] to corrode specimens at USAF-AFRL will be tested in this section to confirm that it can produce a similar type and extent of corrosion on both the low and high-k_t specimens. This size distribution of the resulting corrosion will be compared to that obtained by Sharp using the same protocol.
4. **Machining of Fatigue Specimens:** Low and high-k_t fatigue specimens of the designs used in the SICAS project [4, 5] and by Sharp [3], respectively, will be machined from a plate of AA7050-T7451.
5. **Corrosion of Fatigue Specimens:** Most of the fatigue specimens will be corroded using the corrosion protocol from Crawford and Sharp [3]. The remaining fatigue specimens will be left in the as-machined state.
6. **Fatigue Testing:** Most of the low and high-k_t fatigue specimens will be fatigue tested using a constant amplitude spectrum. Some of the specimens will be tested using a NASA marker band spectrum [10] to facilitate the measurement of crack growth rate and crack shape development. Fatigue testing will be conducted at three load ratios.
7. **Fractography:** The fracture surfaces of the fractured fatigue specimens will be examined optically and in the scanning electron microscope to measure the size of the initiating features, the size of the final cracks and, on the fatigue crack growth specimens, the spacing of marker bands and fatigue striations.
8. **Development of a Fatigue Crack Growth Dataset:** The marker band and fatigue striation observations from the previous stage will be used to create a fatigue crack growth dataset for the material. This dataset will be in the form of fatigue crack

[3] The purchase order number was DSTO4500823459

growth rates (da/dN) in mm/cycle as a function of applied cyclic stress intensity factor (ΔK) in MPa$\sqrt{m}$.

9. **Formulation of Equivalent Crack Size Distributions:** The fatigue crack growth dataset combined with the constituent particle and corrosion pit size distributions will be used to formulate an ECS distribution for the experimental material.
10. **Monte-Carlo Simulation:** A Monte-Carlo model will be developed to estimate the fatigue lives of the low and high-k_t fatigue specimens tested in this project. The purpose of this model will be to see if the ECS from the low-k_t specimens can be used to accurately predict the fatigue lives of the high-k_t specimens.

Each of the stages listed above are discussed in more detail in separate sections below.

3.3.1 Bulk Cut-up of MX Plate

The AA7050-T7451 rolled plate will be cut-up to produce specimens for low and high-k_t fatigue testing, microstructural characterisation and corrosion protocol development. Figure 7 is a flowchart showing the various specimen types that will be cut from the MX plate. A detailed description of the cut-up of the plate can be found in Appendix B.

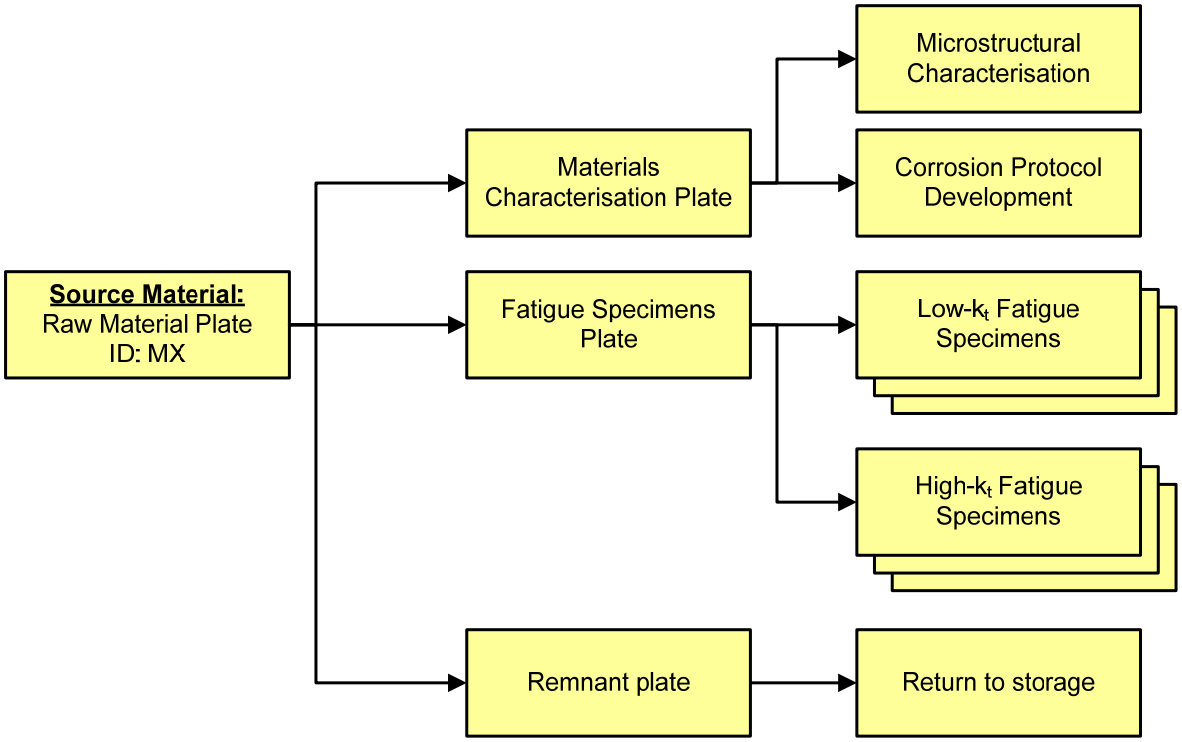

Figure 7: Flowchart of raw material plate cut-up

3.3.2 Microstructural Characterisation

The size distribution of constituent particles in the experimental material as well as the grain size distribution of this material are required to investigate the correlation, if any, between the ECS distribution derived from fatigue testing and the microstructure of the material. The

method described here is similar to that in [11]. Therefore, a vertical slice will be taken from the material[4] to provide microstructural specimens, which will be taken at the material's top and bottom surfaces and at ¼, ½ and ¾ thicknesses in the material. These microstructural specimens will be approximately 10 x 10 x 10 mm cubes. These will be metallographically polished on a single face to a sub-micron quality finish using standard methods to reveal the constituent particles of the material. Specimens will be polished in the L-T, L-S and S-T orientations at each of the positions in the material listed above. There will therefore be three specimens at each of the five positions described above, which gives a total of 15 microstructural specimens.

After each specimen has been polished, micrographs will be taken of a sufficient number of the constituent particles in each orientation and position to allow the development of an extreme value size distribution for the largest constituent particles for each orientation and position. The volume fraction of the particles will also be estimated from the measured area fraction of the particles.

After the constituent particles size distributions and volume fractions have been determined, the specimens will be etched to reveal the alloy's grain structure. The etched specimens will then be examined in the optical microscope to record micrographs of the alloy's grain structure. Sufficient micrographs will be recorded of this microstructure to allow it to be statistically characterised.

3.3.3 Corrosion Protocol Development

A protocol will be developed base on the corrosion protocol used by Sharp [3] during his long term attachment at USAF-AFRL. This protocol consisted of exposing the material to a flowing solution of 3.5 wt% NaCl, which has an initial pH of 11, for 24 hours. This protocol has been selected as its likely effect on AA7050-T7451 is already known and because of its ease of application. Alternative protocols based on the P-3 work on 7075 [12] will be developed if required.

As the Sharp corrosion protocol has not been tested on the low-k_t fatigue specimens, tests will be conducted to determine if the pit size distributions obtained from each specimen type are acceptably similar. This will require the machining of dummy specimens in low and high-k_t geometries. The engineering drawings for each of these dummy specimen types are shown in Figure 8 while Figure 9 compares the orientation of the low and high-k_t specimens. The low-k_t corrosion protocol test specimens will have an exposed surface area equal to the surface area of the hole in the high-k_t coupons. If the difference between the corrosion on the two types of specimens is unacceptable then the protocol used on the low-k_t coupons will be modified. A non-circulating corrosive medium will be trialled initially with the low-k_t specimens but if this does not produce acceptable results then a flowing solution will be used.

[4] See Appendix B for the dimensions and location of this vertical slice in the material plate

a)

b)

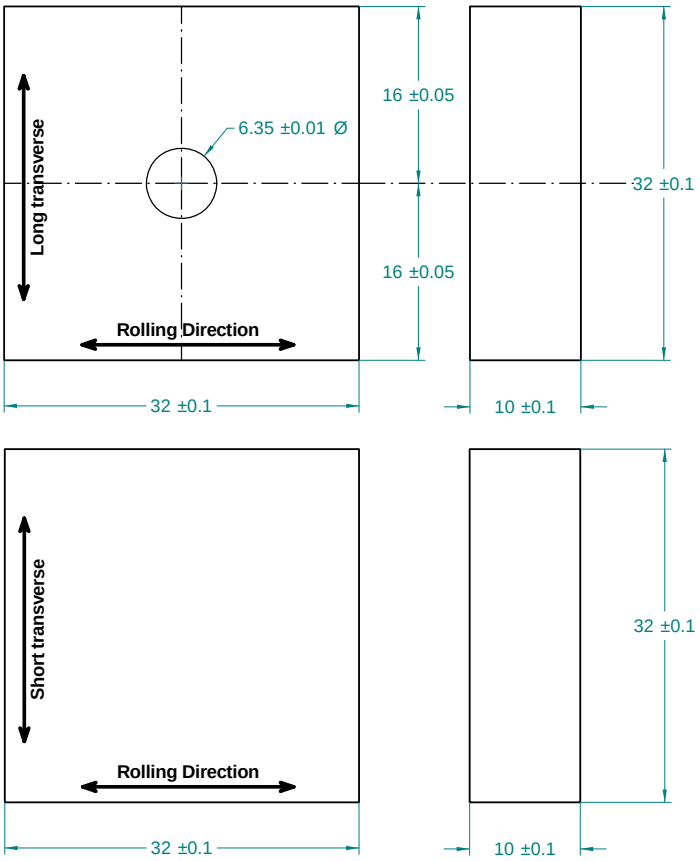

Figure 8: Engineering drawings of (a) high-k_t corrosion protocol dummy specimen and (b) low-k_t corrosion protocol dummy specimen. Note, as indicated by the arrows on each part of the figure, that the orientations of the low and high-k_t specimens are different.

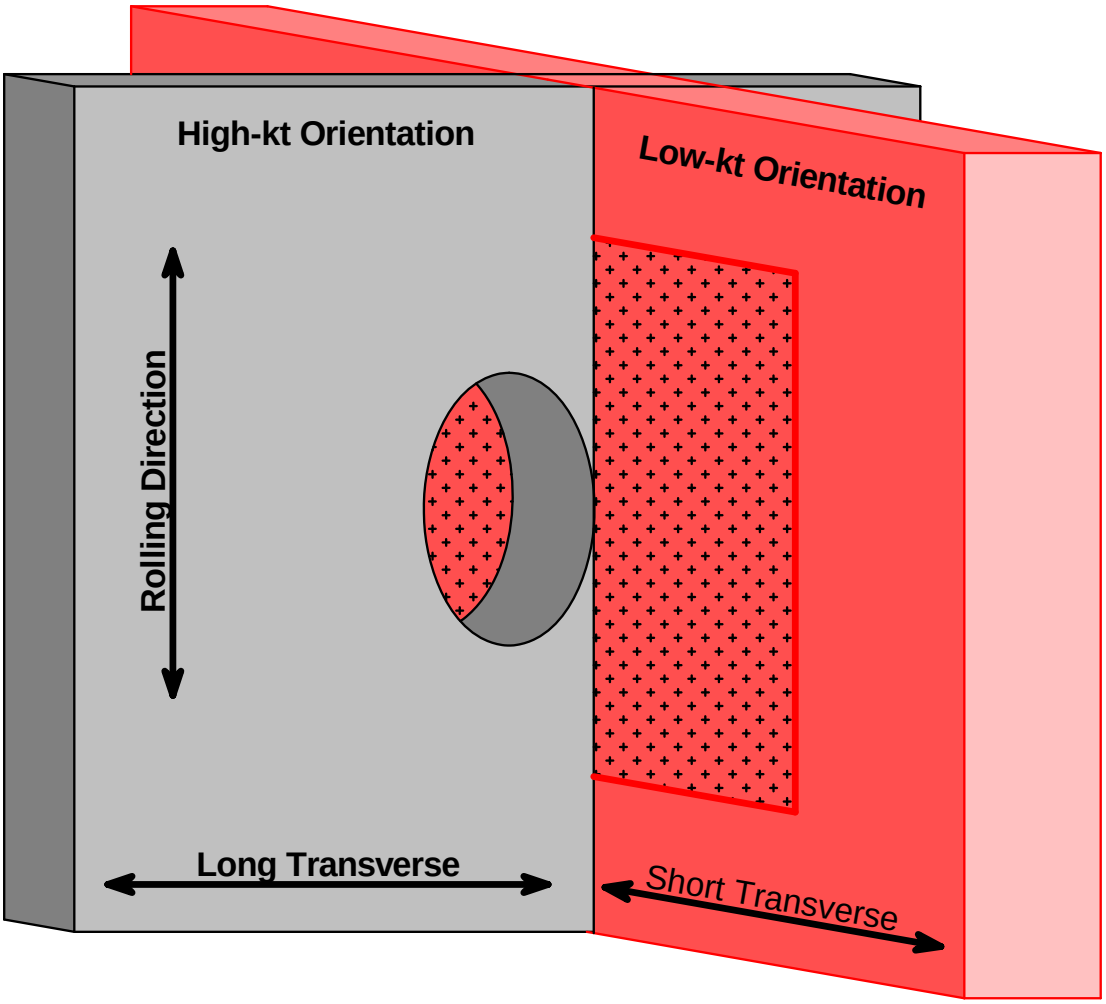

Figure 9: Comparison of the orientations of the high and low-k_t corrosion protocol specimens. In each case, the exposed surface of the microstructure is the same. The corroded region on the low-k_t specimen is shown by the area marked by crosses. The corroded area on the high-k_t specimen is the bore of the hole in the specimen. Note that the fatigue specimens are loaded parallel to the rolling direction during testing.

3.3.4 Machining of Fatigue Specimens

The fatigue crack growth and fatigue life testing in this project will be conducted using both high and low-k_t coupons. This will allow the effect of stress gradients on the ECS methodology to be examined. Specimens will be machined so as to expose the end grain with elongated stringers (L-S plane) on the surface to be corroded.

The next two subsections describe the low and high-k_t specimens that will be used in this work. Appendix B provides detailed drawings of these specimens and cut-up diagrams for their machining from the MX material plate.

3.3.4.1 *Low-k_t Specimens*

The low-k_t fatigue life specimens will be similar to those used in the SICAS project [4, 5] which conformed with ASTM E466 [13]. The current specimens are narrower than the original SICAS specimens to allow two specimens to be machined from the 152.4 mm thickness of the raw material plate. This specimen geometry is shown in Figure 10. The elastic stress concentration factor of this specimen, according to a finite element model [14] was 1.047 which compared well with a handbook solution of 1.041 [15]. A more detailed drawing of the specimen can be found in Appendix B.

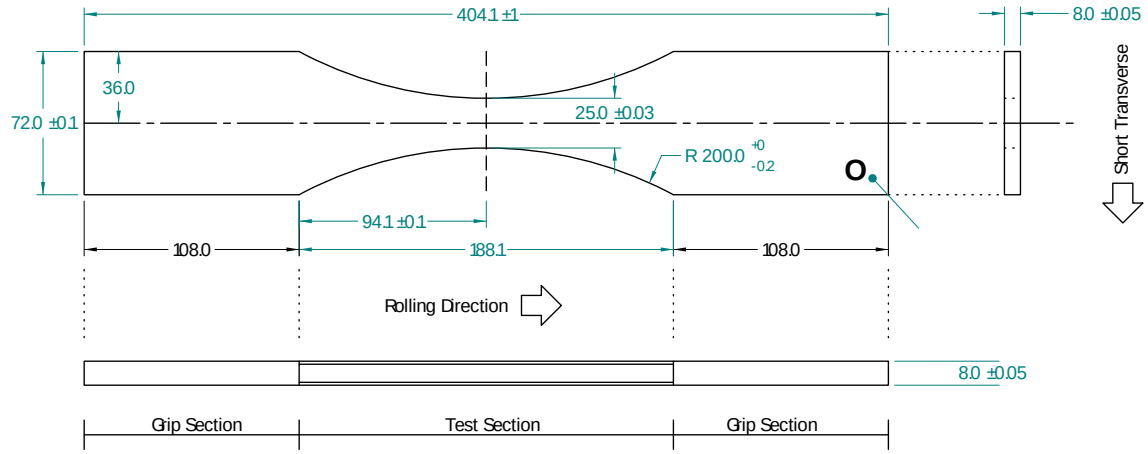

Figure 10: Engineering drawing of the SICAS low-k_t dogbone fatigue specimen. Dimensions are in millimetres.

For these specimens the loading direction will be rolling direction of the plate (L) while the specimen transverse direction will be the plate's short-transverse direction (S). Not all of the low-k_t specimens will be corroded prior to testing. The uncorroded low-k_t specimens will be peened on their corners and sides to prevent fatigue initiation from these locations. Peening will be conducted using the F/A-18 rework peening method developed by DSTO [15].

3.3.4.2 *High-k_t Specimens*

The high-k_t fatigue specimens are of the same design as those used by Sharp during his long term attachment at USAF-AFRL. Their geometry is shown in Figure 11. The specimens will be 32 mm wide and 10 mm thick with a 6.35 mm diameter hole in the middle of their gauge section. The stress concentration factor of these specimens was estimated as 3.15 using the solution from [8]. For these specimens the loading direction will be rolling direction of the plate (L) while the specimen transverse direction will be the plate's long-transverse direction (T).

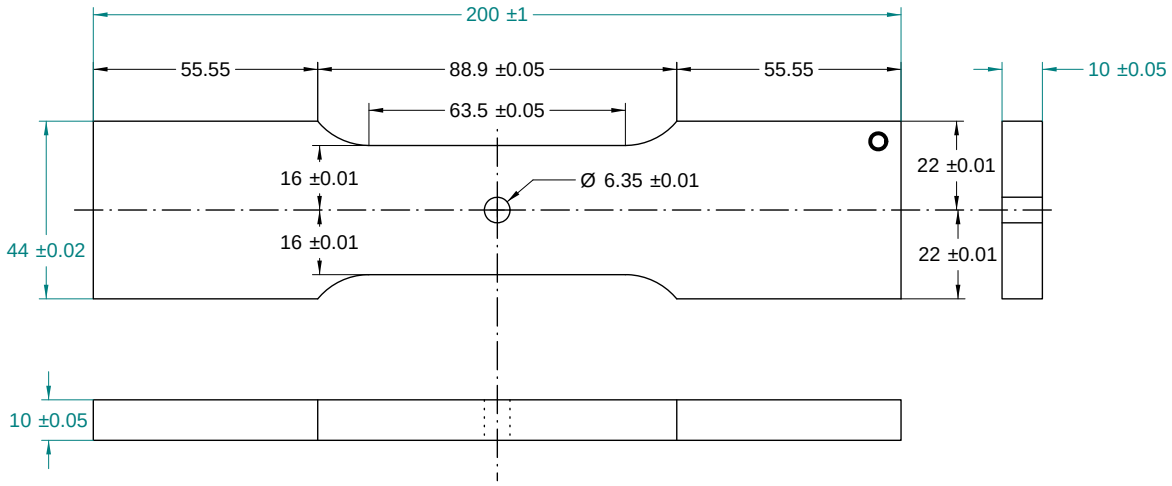

Figure 11: Engineering drawing of the high-k_t fatigue test specimens used in this work. Dimensions are in millimetres.

3.3.5 Corrosion of Fatigue Specimens

The aim in corroding the fatigue specimens is to produce as a similar degree and morphology of corrosion on both the high and low-k_t specimens. One measure to achieve this will be to make the corroded regions on both specimen types of equal area. The corroded area on the high-k_t specimens is the bore of the hole, which has an area of:

$$A_{hole} = 2\pi rb = 2\pi(6.35/2)(10) = 199.5\,\text{mm}^2 \qquad (2)$$

Where r is the radius of the hole and b is the thickness of the high-k_t specimen.

For the low-k_t coupons, this area of corrosion is equivalent to an 8 mm radius (16 mm diameter) circle or a 14.1 x 14.1 mm square. Either shape of corrosion area is acceptable.

For the high-k_t specimens a corrosion treatment rig resembling that used by Crawford and Sharp [3]will be used. The rig required for the low-k_t coupons will be developed once the corrosion protocol for these specimens has been finalised.

Once a specimen has been corroded an aqueous solution of HNO_3 [16] will be used to clean the corroded region. The specimen will then be dried in an oven at 50 °C for 24 hours, allowed to cool in a dry environment and then stored in a desiccator or similar until it is tested.

3.3.6 Fatigue Testing

3.3.6.1 Experimental Matrix

The fatigue testing in this program will consist of both fatigue crack growth tests and fatigue life tests. These tests will be conducted on both low and high-k_t specimens. Table 4 is the experimental matrix for testing of the low-k_t specimens and Table 5 is the experimental matrix for the high-k_t specimens. These tables divide the experimental matrix into several different test series. Three kinds of test will be conducted for each specimen geometry. These are:

1. **Life Scoping Tests:** The fatigue life tests will be conducted on both low and high-k_t specimens under constant amplitude conditions. The applied stresses used in testing have been selected so that the maximum stress in the low and high-k_t specimens is equal. Tests will be conducted at maximum stresses ranging between 26% and 105% of the material's yield stress. The ratio of the stress concentration factors of the high and low-k_t specimen geometries is:

$$\frac{k_{t,high}}{k_{t,low}} = \frac{3.146}{1.041} = 3.004 \approx 3 \qquad (3)$$

   Therefore, the applied stresses on the low-k_t specimens will be three times those applied to the high-k_t specimens.

2. **Fatigue Crack Growth Tests:** The fatigue crack growth tests will be conducted on high and low-k_t specimens using the modified NASA 4-6-10 marker banding spectrum [10] from the SICAS project [4, 5]. Fatigue crack growth rates will be determined after testing by fractographic analysis of the marker bands and of any striations observed.

3. **ECS Tests:** These tests will be conducted on the low and high-k_t specimens at set applied stress levels. The high-k_t specimens will be tested at three applied stress levels while the low-k_t specimens will be tested at four levels. These levels have been selected to give the same maximum stresses in the high and low-k_t specimens. Table 6 shows the correspondence between the stress levels for low and high-k_t tests series. Note that low-k_t ECS test series LCC4 has no corresponding high-k_t ECS test series. Previous experience in testing high-k_t specimens suggests that no fatigue failures would occur at this stress level [3].

3.3.6.2 Fatigue Specimen Randomisation

The specimens in each of the series in Table 4 and Table 5 should come from uniformly distributed positions in the MX material plate. This is to avoid introducing systematic errors due to, for example, selecting all the specimens in a given test series from the same volume of the raw material. This randomisation is to be done prior to the start of testing and each specimens should have a test series identification engraved with a serial number on both its ends. For example, the fifth specimen to be tested in the low-k_t life scoping test series LAC will be engraved LAC-5.

Table 4: Experimental Matrix for Low-k_t Fatigue Specimens

Type	Test Series	Surface Condition	*R*	$\sigma_{applied}$ (MPa)	Replicates	Notes
Life Scoping	LAU	Uncorroded	0.1	Various	10 each (20 total)	Constant amplitude loading
	LAC	Corroded				
FCG	LBU1	Uncorroded	-0.3	Various	8 each (24 total)	Tests will be conducted using the modified NASA 4-6-10 marker banding spectrum [10] used in SICAS [4, 5]
	LBU2	Uncorroded	0.1			
	LBU3	Uncorroded	0.5			
	LBC1	Corroded	-0.3	Various	8 each (24 total)	
	LBC2	Corroded	0.1			
	LBC3	Corroded	0.5			
ECS	LCC1	Corroded	0.1	434	11 each (44 total)	Constant amplitude loading
	LCC2	Corroded		310		
	LCC3	Corroded		207		
	LCC4	Corroded		108		
Total					**112**	

Table 5: Experimental Matrix for High-k_t Fatigue Specimens

Type	Test Series	Surface Condition	*R*	$\sigma_{applied}$ (MPa)	Replicates	Notes
Life Scoping	HAU	Uncorroded	0.1	Various	7 each (14 total)	Constant amplitude loading
	HAC	Corroded				
FCG	HBU	Uncorroded	0.1	Various	6	Modified NASA spectrum (see Table 4)
	HBC	Corroded			7	
ECS	HCC1	Corroded	0.1	144.7	11 each (33 total)	Constant amplitude loading
	HCC2			103.3		
	HCC3			69.0		
Total					**60**	

Table 6: Correspondence between the stress levels for the low and high-k_t ECS test series

σ_{max} (MPa)	Low-k_t		High-k_t	
	Test Series	$\sigma_{applied}$ **(MPa)**	**Test Series**	$\sigma_{applied}$ **(MPa)**
434	LCC1	434.0	HCC1	144.7
310	LCC2	310.0	HCC2	103.3
207	LCC3	207.0	HCC3	69.0
108	LCC4	108.0	–	–

3.3.6.3 Environmental Control During Fatigue Testing

Wei has shown that humidity strongly affects fatigue crack growth rates (Figure 12) [17]. Examination of Figure 3.7.4.2.9(a) in the Metallic Materials Properties Development and Standardization handbook [7] shows that there is no effect of humidity on the fatigue crack growth of 3.15 inch thick AA7050-T7451 plate between humidities of 50% and 100% RH, which is within humidity range of the upper plateau in Figure 12. This means that fatigue testing should be conducted in a controlled humidity environment. In the SICAS project a high humidity environment was used as it was easier to produce and control a high humidity environment than a low humidity environment. In addition, fatigue crack growth rates are higher at higher humidities [17] which leads to shorter and therefore conservative fatigue lives. The same practice will be used in the current project. The high humidities will be created by sealing the gauge section of the specimens in a humidity control chamber during fatigue testing. The low-k_t specimens will be tested using the humidity control chambers and methods created for the SICAS project [4, 5]. A new pair of chambers will need to be made for the high-k_t specimens due to their smaller size. The performance of both types of chambers will be tested to ensure that approximately the same relative humidity is present in both chambers during fatigue testing.

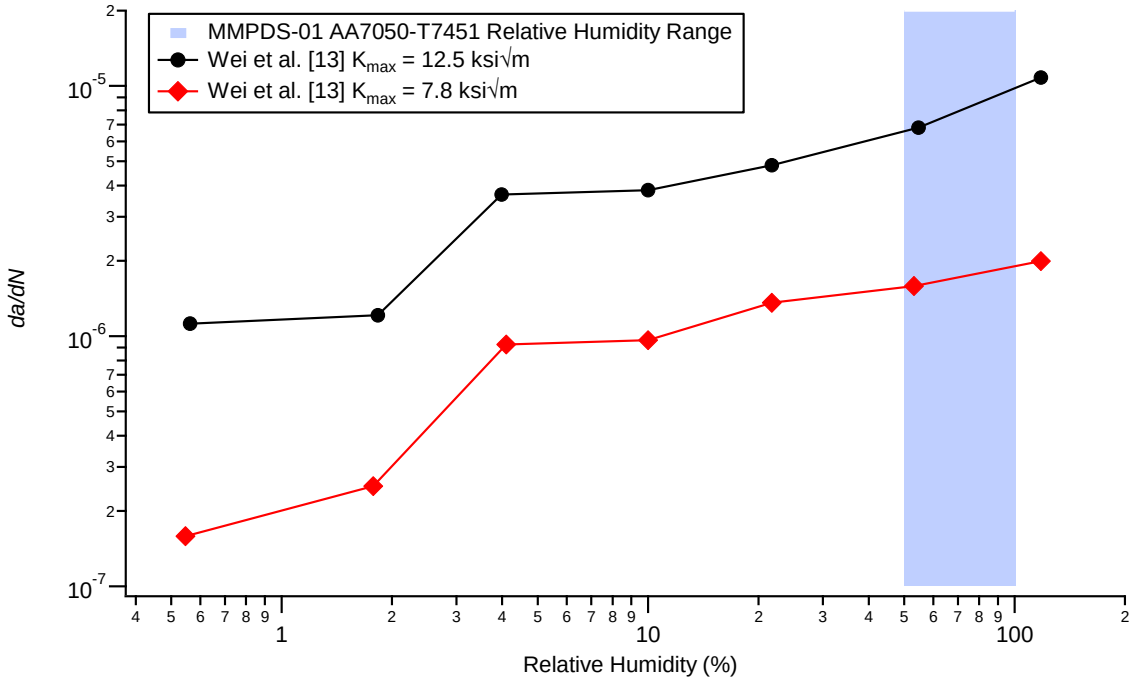

Figure 12: Effect of moisture content on Al-Zn-Mg alloy fatigue crack growth rate (f = 57 Hz) from Wei [17] and range of relative humidities of fatigue crack growth data from MMPDS-01 [7]

3.3.6.4 *Reporting*

As the work in this experimental plan is intended for use in certification, all fatigue test results will be reported in National Association of Testing Authorities (NATA) approved reports. Test plans will need to be submitted to the management of the Fatigue and Fracture Laboratory at DSTO Melbourne prior to testing. These plans will form part of the NATA approved reporting of the test results.

In addition, the pages of the laboratory note books used to record the set-up and results of these tests will be scanned and added to the report containing the results from these fatigue tests.

3.3.7 Fractography

Once a specimen has been tested, and assuming it has failed, its fracture surface will be removed using an abrasive cut-off wheel, cleaned using an aqueous nitric acid solution (HNO_3) [16] and examined in both the optical and scanning electron microscopes (SEM). Micrographs will be recorded of the initiating defect (or defects) using the SEM. These micrographs will be analysed to determine the size of the initiating defect in terms of its projected width, depth and area on the fracture surface. This information will subsequently be used in developing the equivalent crack size distributions for the low and high-k_t coupons.

The fatigue crack growth specimens will be examined to locate the marker bands using an optical microscope with a long working distance objective lens and an instrumented stage. The position of the markers bands with respect to the origin of the crack will be measured

using the instrumented stage. Where possible the shape of the crack front will be mapped using the marker bands. The position of the marker bands relative to the initiating defect will be used to calculate the cyclic stress intensity factor for the crack. This will be combined with the crack growth rate data obtained from the separation of the marker bands and from striation measurements to create a set of low and high-k_t fatigue crack growth data. This above method has previously been used in the SICAS project [4, 5].

3.3.8 Development of a Fatigue Crack Growth Dataset

The marker band and fatigue striation observations from the previous stage will be used to create a fatigue crack growth dataset for the material. The position of the marker bands will be used to calculate both the distance of the marker band from the surface while the separation between adjacent marker bands will be used to calculate average crack growth rates. This method was previously used to develop the 'Marker Band' dataset used in the SICAS project [4, 5].

The stress intensity factors for a given point on a marker band will be calculated using the Newman and Raju solutions for semi-elliptical surface cracks and double semi-elliptical cracks in a hole bore [18]. As in the SICAS project, it will be assumed that there is no fatigue threshold.

3.3.9 Formulation of Equivalent Crack Size Distributions

In this stage, the fatigue crack growth data from the previous stage will be combined with the fractography data to create equivalent crack size distribution for the uncorroded and corroded states of both the low and high-k_t specimens. In the first instance, this will be achieved using the method described in the SICAS final report [4] which used the fatigue crack growth prediction package AFGROW. This method fed initial crack size estimates, material, geometry and loading conditions into an AFGROW model. AFGROW was then allowed to predict the number of cycles to failure and final crack length. The predicted number of cycles to failure was then compared to the actual (i.e. experimentally obtained) fatigue life and the initial crack size estimate was adjusted accordingly. This process was repeated until the difference between the actual and predicted fatigue lives was less than 1%. The resultant distribution of initial crack sizes is the equivalent crack size distribution. If time allows the above process will be repeated using FASTRAN as implemented using the DSTO software package CGAP [19].

3.3.10 Monte Carlo Simulation

The fatigue crack growth data obtained in Section 3.3.8 will be combined with ECS distribution calculated in Section 3.3.9 using a Monte Carlo simulation. A similar model for AA7010-T7651 has previously been developed by Crawford et al. [20]. This earlier model was used to predict how pitting corrosion affected the location of fatigue failures in a low-k_t fatigue specimen. The model from this previous work will be adapted to the current work by inserting the FCG data derived from marker band observation and the ECS distribution developed from fractography.

4. Summary

The expected outcomes of this work are:

1. two pit size distributions for the aluminium alloy AA7050-T7451;
2. grain size distributions for the alloy in the three principal material planes;
3. two equivalent crack size distributions for the corroded AA7050-T7451 tested under low and high-k_t conditions; and
4. a Monte Carlo simulation to determine if the low-k_t ECS distribution for corroded AA7050-T7451 can be used to predict the fatigue life of the corroded high-k_t fatigue specimens.

Comparison of the equivalent crack size distributions and Monte Carlo simulations results obtained for the low and high-k_t specimens will quantify the effect of the different stress gradients in each specimen type on fatigue life. If successful, this will allow ECS distributions from low-k_t specimens to be used under high-k_t conditions such as near a fastener hole. This will greatly simplify subsequent modelling work.

5. References

1. *Technical Airworthiness Management Manual*. (2005) 7001.053(AM1), RAAF Base Williams, Directorate General Technical Airworthiness
2. Crawford, B. R., Loader, C. and Sharp, P. K. (2010) *A Proposed Roadmap for Transitioning DSTO's Corrosion Structural Integrity Research into Australian Defence Force Service*. DSTO-TR-2475, [Technical Report] Melbourne, Defence Science and Technology Organisation
3. Crawford, B. R. and Sharp, P. K. (2011) *ECS Modelling of 7050 Aluminium Alloy Corrosion Pitting and its Implications for Aircraft Structural Integrity*. Unpublished, Melbourne, Defence Science and Technology Organisation
4. Crawford, B. R., et al. (2005) *Structural Integrity Assessment of Corrosion in Aircraft Structures*. DSTO-RR-0294, Melbourne, Defence Science and Technology Organisation
5. Crawford, B. R., et al. (2005) The EIFS distribution for anodized and pre-corroded 7010-T7651 under constant amplitude loading. *Fatigue and Fracture of Engineering Materials and Structures* **28** (9) 795-808
6. Crawford, B. R., et al. (2012) *Fatigue Life Testing of Surface Grain Corroded 7050-T7451*. Unpublished, Melbourne, Melbourne, Defence Science and Technology Organisation
7. *Metallic Materials Properties Development and Standardization (MMPDS)*. (2003) DOT/FAA/AR-MMPDS-01, Springfield, VA, U.S. Department of Transportation
8. Pilkey, W. D. (1997) *Peterson's Stress Concentration Factors*. 2nd ed. New York, John Wiley and Sons

9. Taylor, D. (2011) *RE: Materials Register [SEC=UNCLASSIFIED]*. Personal Communication to: Crawford, B. R., Melbourne, Defence Science and Technology Organisation
10. Willard, S. A. (1997) *Use of Marker Bands for Determination of Fatigue Crack Growth Rates and Crack Front Shapes in Pre-Corroded Coupons*. NASA/CR-97-206291, Hampton, NASA
11. Merati, A. (2005) A study of nucleation and fatigue behavior of an aerospace aluminum alloy 2024-T3. *International Journal of Fatigue* **27** (1) 2005/1 33-44
12. Shekhter, A., et al. (2007) *Assessment of the effect of pitting corrosion on the safe life prediction of the P3-C*. DSTO-TR-2080, [Technical Report] Defence Science and Technology Organisation
13. ASTM (2002) E466-96(2002)e1 Standard Practice for Conducting Force Controlled Constant Amplitude Axial Fatigue Tests of Metallic Materials. In: *ASTM Annual Book of Standards*. Vol. 03.01, Philadelphia, ASTM
14. Urbani, C. (2004) *Analysis by FEM of fatigue test coupon (a work in progress)*. Melbourne. CSIRO: p. 13.
15. Young, W. C. (1989) *Roark's Formulas for Stress & Strain*. 6th ed. New York, McGraw-Hill
16. G1-90(1999)e1 Standard Practice for Preparing, Cleaning, and Evaluating Corrosion Test Specimens. (1999) In: *ASTM Annual Book of Standards*. Vol. 03.02. Philadelphia 15-21
17. Wei, R. P. (1970) Some aspects of environment-enhanced fatigue-crack growth. *Engineering Fracture Mechanics* **1** (4) 633-651
18. Newman, J. C. and Raju, I. S. (1986) Stress Intensity Factor Equations for Cracks in Three-Dimensional Bodies Subjected to Tension and Bending Loads. In: *Computational Methods in the Mechanics of Fracture*. Elsevier Science Publishers B.V.
19. Hu, W. and Wallbrink, C. (2010) *A Strain-Life Module for CGAP: Theory, User Guide and Examples*. DSTO-TR-2392, Melbourne, Defence Science and Technology Organisation
20. Crawford, B. R., Loader, C. and Sharp, P. K. (2004) The Effect Of Pitting Corrosion On The Position Of Aircraft Structural Failures. In: *Structural Integrity and Fracture,* Brisbane, Australia: 26-29 September, 2004

Appendix A: Material Conformity Certificate

Aleris Aluminum Koblenz GmbH
Carl-Spaeter Str.10 56070 Koblenz/Deutschland

Aleris Europe

INSPECTION CERTIFICATE (EN 10204/3.1) / TEST REPORT / APPROVED CERTIFICATE

NO.: 0272783 SERIAL-NO.: PAGE: 1 / 6

PURCHASER: THYSSENKRUPP AEROSPACE
AUSTRALIA PTY LTD

7-10 DENOCI CLOSE
AUS WETHERILL PARK,NSW 2164

CONSIGNEE: THYSSEN KRUPP AEROSPACE
PTY LTD

UNIT 2, 7-10 DENOCI CLOSE
AUS WETHERILL PARK,NSW 2164

ORDER NO. PURCHASER: T06170 ITEM 06

PART NO. PURCHASER:

ORDER NO. MANUFACTURER/ITEM: 56963 / 06

PRODUCT: PLATE

SPECIFICATION: AM+BA+BM I+DM+MM+EOF

ALLOY/TEMPER: 7050 T7451

DIMENSION: 152,40 x 1220,00 x 3660,00 mm

PCS.	GROSS KG	NET KG	PACK-NO	LOT-NO
1	2.044	1.954	676411	398903
1	2.025	1.953	676598	398902

WT-TO-QS 07/09

Aleris Aluminum Koblenz GmbH
Carl-Spaeter Str.10 56070 Koblenz/Deutschland

Aleris Europe

INSPECTION CERTIFICATE (EN 10204/3.1) / TEST REPORT / APPROVED CERTIFICATE

NO.: 0272783 LOT: 398903 PAGE: 2 / 6

RESULTS:

Mechanical properties:

Pl.	No.	Spec. No.	Y.S. N/mm²	U.T.S. N/mm²	El. %		K1C 1/2 MPam
Min. LT:			414	483	4,0	Min. T-L:	24,20
Max. LT:						Max. T-L:	
1	A		430	505	9,39		32,20
1	E		431	506	9,43		
Min. L:			414	483	8,0	Min. L-T:	26,40
Max. L:						Max. L-T:	
1	A		440	501	10,7		
1	E		441	502	10,8		35,30
Min. ST:			393	462	3,0	Min. S-L:	23,10
Max. ST:						Max. S-L:	
1	A		412	490	5,61		35,20
1	E		408	484	5,77		

Chemical composition: in % , remainder Al Cast No.: 5-11-2160

Si	Fe	Cu	Mn	Mg	Cr	Zn	Ti	B
0,030	0,046	2,194	0,000	2,058	0,000	6,224	0,0303	0,0004
Zr	Pb	Ni	Sn	Be	Na	Li	V	H2 (*)
0,1043	0,0019	0,0039	0,0042	0,0002	0,0000	0,0000	0,0065	0,05
Al	Tl	Ti+Zr	Cu/Mg	Fe/Si				
		0,135		1,5				

(*) = H2 in ml/100 g AL

Other tests:

Dimensional check:	OK	
Surface control:	OK	
Ultrasonic test:	OK	US-spec.: ASTM+BSS+GS+AM+PS+GA+Mil

WT-TQ-QS 07/08

Normative references:

LEGIERUNGSNORM/CHEMICAL COMPOSITION STANDARD/COMPOSITION CHIMIQUE
AMS 4050 H
FESTIGKEITSNORM/MECH. PROP.STANDARD/CARACTERISTIQUE MECANIQUE
AMS 4050H+BAMS 516-003 REV.NC+BMS 7-323D TYPE I+

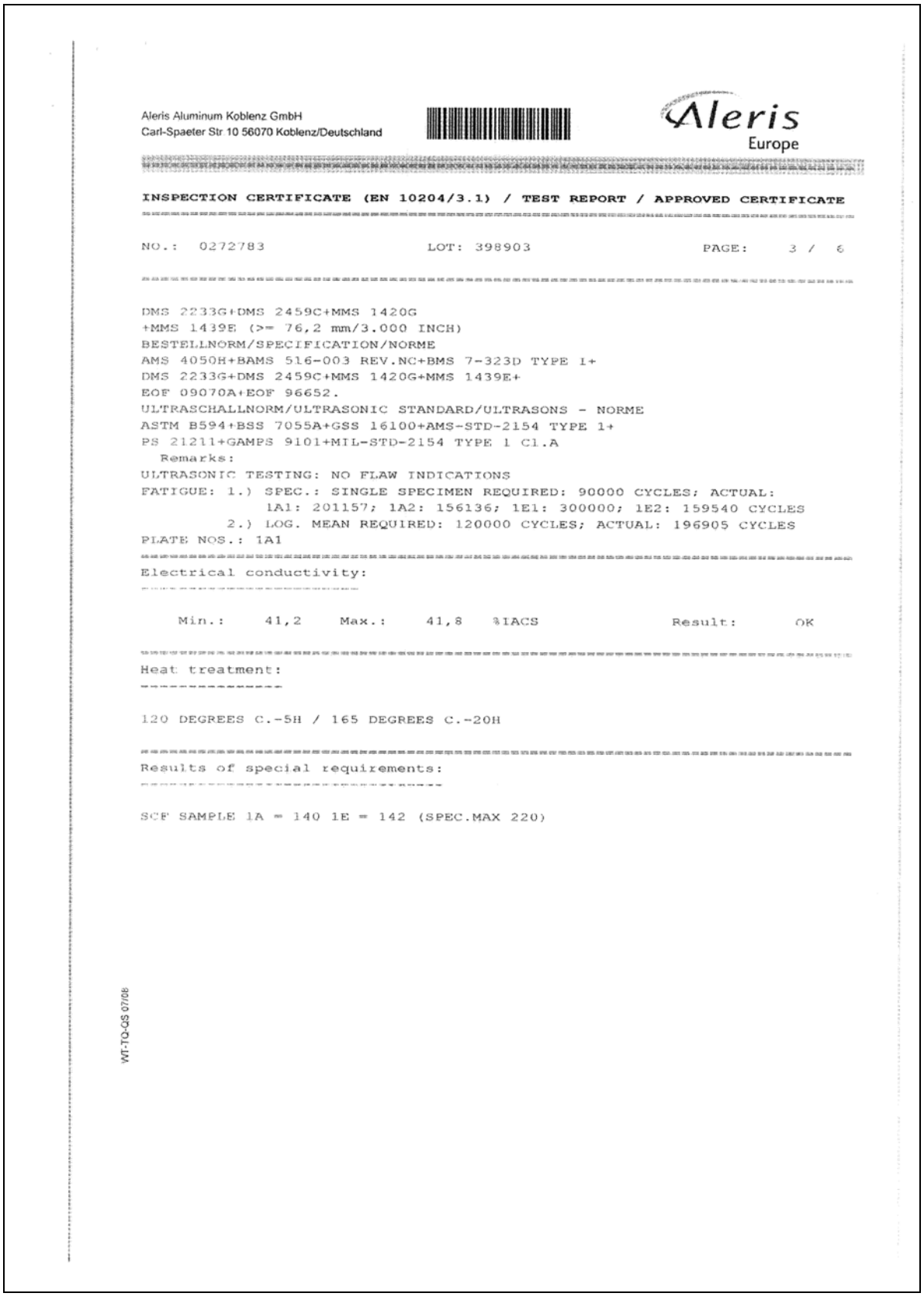

Aleris Aluminum Koblenz GmbH
Carl-Spaeter Str 10 56070 Koblenz/Deutschland

Aleris Europe

INSPECTION CERTIFICATE (EN 10204/3.1) / TEST REPORT / APPROVED CERTIFICATE

NO.: 0272783 LOT: 398903 PAGE: 3 / 6

DMS 2233G+DMS 2459C+MMS 1420G
+MMS 1439E (>= 76,2 mm/3.000 INCH)
BESTELLNORM/SPECIFICATION/NORME
AMS 4050H+BAMS 516-003 REV.NC+BMS 7-323D TYPE 1+
DMS 2233G+DMS 2459C+MMS 1420G+MMS 1439E+
EOF 09070A+EOF 96652.
ULTRASCHALLNORM/ULTRASONIC STANDARD/ULTRASONS - NORME
ASTM B594+BSS 7055A+GSS 16100+AMS-STD-2154 TYPE 1+
PS 21211+GAMPS 9101+MIL-STD-2154 TYPE 1 Cl.A
Remarks:
ULTRASONIC TESTING: NO FLAW INDICATIONS
FATIGUE: 1.) SPEC.: SINGLE SPECIMEN REQUIRED: 90000 CYCLES; ACTUAL:
1A1: 201157; 1A2: 156136; 1E1: 300000; 1E2: 159540 CYCLES
2.) LOG. MEAN REQUIRED: 120000 CYCLES; ACTUAL: 196905 CYCLES
PLATE NOS.: 1A1

Electrical conductivity:

Min.: 41,2 Max.: 41,8 %IACS Result: OK

Heat treatment:

120 DEGREES C.-5H / 165 DEGREES C.-20H

Results of special requirements:

SCF SAMPLE 1A = 140 1E = 142 (SPEC.MAX 220)

WT-TQ-QS 07/08

Aleris Aluminum Koblenz GmbH
Carl-Spaeter Str 10 56070 Koblenz/Deutschland

Aleris Europe

INSPECTION CERTIFICATE (EN 10204/3.1) / TEST REPORT / APPROVED CERTIFICATE

NO.: 0272783 LOT: 398902 PAGE: 4 / 6

RESULTS:

Mechanical properties:

Pl.	No.	Spec. No.	Y.S. N/mm²	U.T.S. N/mm²	El. %		K1C 1/2 MPam
Min. LT:			414	483	4,0	Min. T-L:	24,20
Max. LT:						Max. T-L:	
	1	A	432	506	9,68		32,40
	1	E	431	506	9,03		
Min. L:			414	483	8,0	Min. L-T:	26,40
Max. L:						Max. L-T:	
	1	A	441	501	11,1		
	1	E	442	502	10,9		34,30
Min. ST:			393	462	3,0	Min. S-L:	23,10
Max. ST:						Max. S-L:	
	1	A	411	489	5,22		32,20
	1	E	412	490	5,30		

Chemical composition: in % , remainder Al Cast No.: 5-11-2160

Si	Fe	Cu	Mn	Mg	Cr	Zn	Ti	B
0,030	0,046	2,194	0,000	2,058	0,000	6,224	0,0303	0,0004
Zr	Pb	Ni	Sn	Be	Na	Li	V	H2 (*)
0,1043	0,0019	0,0039	0,0042	0,0002	0,0000	0,0000	0,0065	0,05
Al	Tl	Ti+Zr	Cu/Mg	Fe/Si				
		0,135		1,5				

(*) = H2 in ml/100 g AL

Other tests:

Dimensional check: OK
Surface control: OK
Ultrasonic test: OK US-spec.: ASTM+BSS+GS+AM+PS+GA+Mil

Receive As TKA A number A19824
Date: 28 APR 2011 Stamp: 53 CAT A TKA

WT-TQ-QS 07/06

Normative references:

LEGIERUNGSNORM/CHEMICAL COMPOSITION STANDARD/COMPOSITION CHIMIQUE
AMS 4050 H
FESTIGKEITSNORM/MECH. PROP.STANDARD/CARACTERISTIQUE MECANIQUE
AMS 4050H+BAMS 516-003 REV.NC+BMS 7-323D TYPE I+

Aleris Aluminum Koblenz GmbH
Carl-Spaeter Str 10 56070 Koblenz/Deutschland

Aleris Europe

INSPECTION CERTIFICATE (EN 10204/3.1) / TEST REPORT / APPROVED CERTIFICATE

NO.: 0272783 LOT: 398902 PAGE: 5 / 6

DMS 2233G+DMS 2459C+MMS 1420G
+MMS 1439E (>= 76,2 mm/3.000 INCH)
BESTELLNORM/SPECIFICATION/NORME
AMS 4050H+BAMS 516-003 REV.NC+BMS 7-323D TYPE I+
DMS 2233G+DMS 2459C+MMS 1420G+MMS 1439E+
EOF 09070A+EOF 96652.
ULTRASCHALLNORM/ULTRASONIC STANDARD/ULTRASONS - NORME
ASTM B594+BSS 7055A+GSS 16100+AMS-STD-2154 TYPE 1+
PS 21211+GAMPS 9101+MIL-STD-2154 TYPE 1 Cl.A
Remarks:
ULTRASONIC TESTING: NO FLAW INDICATIONS
FATIGUE: 1.) SPEC.: SINGLE SPECIMEN REQUIRED: 90000 CYCLES; ACTUAL:
1A1: 133019; 1A2: 124344; 1E1: 300000; 1E2: 300000 CYCLES
2.) LOG. MEAN REQUIRED: 120000 CYCLES; ACTUAL: 196424 CYCLES
PLATE NOS.: 1A1

Electrical conductivity:

Min.: 42,2 Max.: 42,8 %IACS Result: OK

Heat treatment:

120 DEGREES C.-5H / 165 DEGREES C.-20H

Results of special requirements:

SCF SAMPLE 1A = 137 1E = 136 (SPEC.MAX 220)

WT-TQ-QS 07/08

Aleris Aluminum Koblenz GmbH
Carl-Spaeter Str.10 56070 Koblenz/Deutschland

Aleris Europe

INSPECTION CERTIFICATE (EN 10204/3.1) / TEST REPORT / APPROVED CERTIFICATE

NO.: 0272783 PAGE: 6 / 6

Remarks:

CERTIFIED THAT THE WHOLE OF THE SUPPLIES DETAILED HEREON HAVE BEEN MANUFACTURED, INSPECTED, TESTED AND UNLESS OTHERWISE STATED CONFORM IN ALL RESPECTS TO THE RELEVANT SPECIFICATIONS, DRAWINGS AND CONTRACT/ORDER. WE CONFIRM, THAT QUALITY MANAGEMENT SYSTEM OF ALERIS ALUMINUM KOBLENZ GMBH IS IN ACCORDANCE WITH DIN EN ISO 9001 AND EN 9100 IN THE RELEVANT VALID VERSION AND CERTIFIED BY AN ACCREDITED 3RD PARTY.

MADE IN THE FEDERAL REPUBLIC OF GERMANY

Enclosures:

WT-TQ-QS 07/08

Koblenz, the 17.02.11 PS

P. Gardiner

Patrick Gardiner
Quality assurance

Aleris Aluminum
Koblenz GmbH

Appendix B: Material Cut-Up Diagram

This appendix contains the instructions for the cut-up and machining of the various specimens to be tested in this project. These instructions will be supplied to the machinists to allow them to quote on and undertake the machining.

Cutup Diagram for Machining of Fatigue and Corrosion Coupons from AA7050-T7451

Version 4 (Original written 30/12/2011, Revised 23/01/2012)

Author: Bruce Crawford, AVD, x7751,

Task: LRR 07/250

B.1. Introduction

The following is the cutup diagram for the machining of fatigue and corrosion samples from raw material plate MX. This document accompanies Request for Quote Number X[5].

B.2. Raw Material

The raw material is a rolled plate of aluminium alloy AA7050-T7451 (AMS 4050). This plate is identified as MX in the DSTO-AVD Experimental Materials Register. It is 3660 mm long (rolling direction), 1220 mm wide and 152.4 mm thick. It is illustrated in plan view in Figure 13.

B.3. Cutting Allowances

The diagrams in this plan assume cut thicknesses of 10 mm for coarse cutting (i.e. using a bandsaw) and 2.5 mm for fine cutting (i.e. using an abrasive water jet or EDM milling machine).

B.4. Specimen Identification

The position of each specimen and piece of remnant material machined from the supplied material should be fully traceable. **That is, the exact position of each specimen in the original material must be known.** To achieve this each specimen and remnant piece should be identified according to the identification system described in the cut-up diagrams contained in this document. A machined 'O' mark must be included on the upper left corner of the left end (relative to the plate as illustrated in Figure 13) of the upper grip tab of each fatigue coupon. The Specimen ID should be stamped in each end of the specimen. The specimen ID is to be of the form:

[Material Name][Section Name][Piece Name][Specimen Number]

[5] The number of the Request for Quote will be completed when these cut-up instructions are supplied to a machinist to obtain a quote

Where:

1. Material Name is MX,
2. Section Name is one of A, B or R,
3. Piece Name is:
    a. 1 to 10 for Section A and
    b. 1 to 13 for Section B.
4. Specimen Number is:
    a. A to K for Section A, Pieces A1, A2, A5, A6, A9 and A10,
    b. A to Z and AA to AD for Section A, Pieces A3 and A7,
    c. Blank for Pieces A4 and A8,
    d. M[nn] for metallographic specimens from Section B
    e. CH[n] for high-k_t corrosion specimens from Section B, and
    f. CL[n] for low-k_t corrosion specimens machined from Section B.

B.5. Expected Number of Specimens

It is expected that a total of 112 low-k_t and 60 high-k_t fatigue specimens will be produced using this cutup plan. There will also be one large block of remnant material (Section B) and two smaller pieces (Pieces A3 and A8) which should be returned to DSTO Fishermans Bend.

B.6. Metrology

One-fifth (20%) of the **fatigue** specimens should be selected at random for metrology to ensure conformance to the dimensions and tolerances detailed in the engineering drawings contained in this document.

B.7. Bulk Cutup

The raw material should be cut into blocks as per Figure 13 and Figure 14. The raw material is to be cut into three sections. These are:

- Section A: Fatigue Test Specimens,
- Section B: Microstructural and Corrosion Test Specimens, and
- Section R: Remnant material to be returned to customer without further machining

B.8. Cutup of Section A

B.8.1 Sectioning into Blocks A1 to A10

Figure 14 shows the cut-up of Section A of the raw material into ten blocks labelled A1 to A10. The use and dimensions of each of these blocks are shown in Table 7.

Table 7: Dimensions and use of the pieces A1 to A10 of Section A of Raw Material MX

Pieces (MX-xx)	Use	Dimensions (mm)		
		L	T	S
A1, A2, A5, A6, A9 and A10	High-k_t fatigue coupons in L-T orientation	250	46	152.4
A3 and A7	Low-k_t fatigue coupons in L-S orientation	410	511	152.4
A4 and A8	Reserve pieces for low-k_t fatigue coupons in T-L orientation	90	511	152.4

B.8.2 Cut-up of Blocks A1, A2, A5, A6, A9 and A10

Blocks A1, A2, A5, A6, A9 and A10 are to be machined blanks for high-k_t specimens in the *L-T* orientation as per Figure 15. Ten high-k_t specimens are to be machined from each block. This gives a total of 60 high-k_t specimens from all six blocks. Labels MX-A[n]A to MX-A[n]K should be stamped on the specimen blanks to ensure their traceability during machining. [n] refers to the piece number and is 1, 2, 5, 6, 9 or 10.

B.8.3 Cut-up of Blocks A3 and A7

Blocks A3 and A7 are to be machined blanks for high-k_t specimens in the *L-T* orientation as per Figure 16. 56 specimens are to be machined from each block. This gives a total of 112 specimens from both blocks. Labels MX-A[n]A to MX-A[n]Z and MX-A[n]AA to MX-A[n]AD should be stamped on the specimen blanks to ensure their traceability during machining. [n] refers to the piece number and is either 3 or 7.

B.8.4 Reserve Blocks from Section A

Blocks A4 and A8 from Section A are to be stamped (not engraved) with their identification numbers and microstructural directions and returned to the customer with no further machining. For example, Block A4 should be labelled MX-A4 and marked with arrows indicating the rolling direction and the long transverse direction of the plate.

B.8.5 Machining of High-k_t Specimens

The high-k_t specimen geometry is illustrated as an engineering drawing in Figure 17. This drawing also shows the position of the final specimen within the specimen blanks.

1. A total of 60 specimens will be machined from Blocks A1, A2, A5, A6, A9 and A10.
2. These coupons are 10 mm thick and each blank is at least 12 mm thick. This leaves a maximum machining allowance of 2 mm.
3. The specimens have a flatness tolerance of 0.05 mm. To achieve this fine machining cuts will be required. After each such cut the specimen should be flipped over to

reveal its back face and another cut made. The specimen should be cut and flipped over in this manner until the required thickness of 10.0 mm is achieved.

B.8.6 Machining of Low-k_t Specimens

The low-k_t specimen geometry is illustrated in Figure 18. The positions of the low-k_t specimens in the specimen blanks from Blocks A3 and A7 are shown in Figure 19.

1. A total of 112 low-k_t fatigue specimens will be machined from Blocks A3 and A7
2. These coupons are 8 mm thick and each blank is up to 18 mm thick. This leaves a maximum 10 mm cutting and machining allowance. Some of this will be used up by cutting.
3. The specimens have a flatness tolerance of 0.05 mm. To achieve this fine machining cuts will be required. After each such cut the specimen should be flipped over to reveal its back face and another cut made. The specimen should be cut and flipped over in this manner until the required thickness of 8.0 mm is achieved.

Note the rounding of the specimen corners to a 1.5 mm radius in the gauge section. This rounding continues the entire length of the gauge sections on all four of the gauge section's corners.

B.9. Cut-up of Section B

B.9.1 General Description

Section B of the MX material plate is a 40 mm long vertical slice through the material plate. Specimens will be cut from this plate for microstructural and corrosion tests at the material's top and bottom surfaces and at ¼, ½ and ¾ thicknesses in the material. Figure 21 shows the position of the microstructural and corrosion specimens to be machined from Section B. The cuts shown in this diagram should be used to maximise the amount of remnant material from Section B.

B.9.2 Microstructural Specimens

The microstructural specimens will be 10 x 10 x 10 mm cubes orientated so that their faces correspond to the L-T, L-S and T-S planes of the raw material plate. An engineering drawing of these specimens can be found in Figure 22. This figure shows that the top surface should be labelled with the specimen ID and an arrow indicating the rolling direction of the material.

If there is insufficient room to engrave the specimen with its identification number then each metallographic specimen should be placed in a labelled and sealed plastic bag. In any case, the orientation arrow must be on put on the specimen.

B.9.3 Corrosion Specimens

The corrosion specimens will be machined in high (i.e. with hole) and low-k_t (i.e. without hole) geometries. These geometries are shown in Figure 23. The orientation of these specimens is the same as for the corresponding fatigue specimens.

B.10. Figures

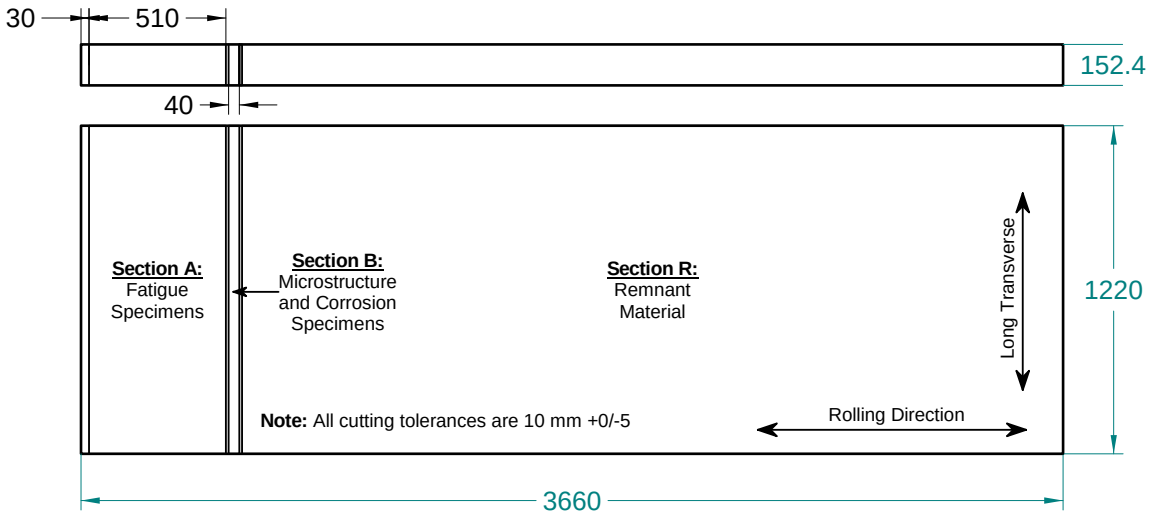

Figure 13: Plan view of bulk cut-up of MX material plate. Dimensions are in millimetres

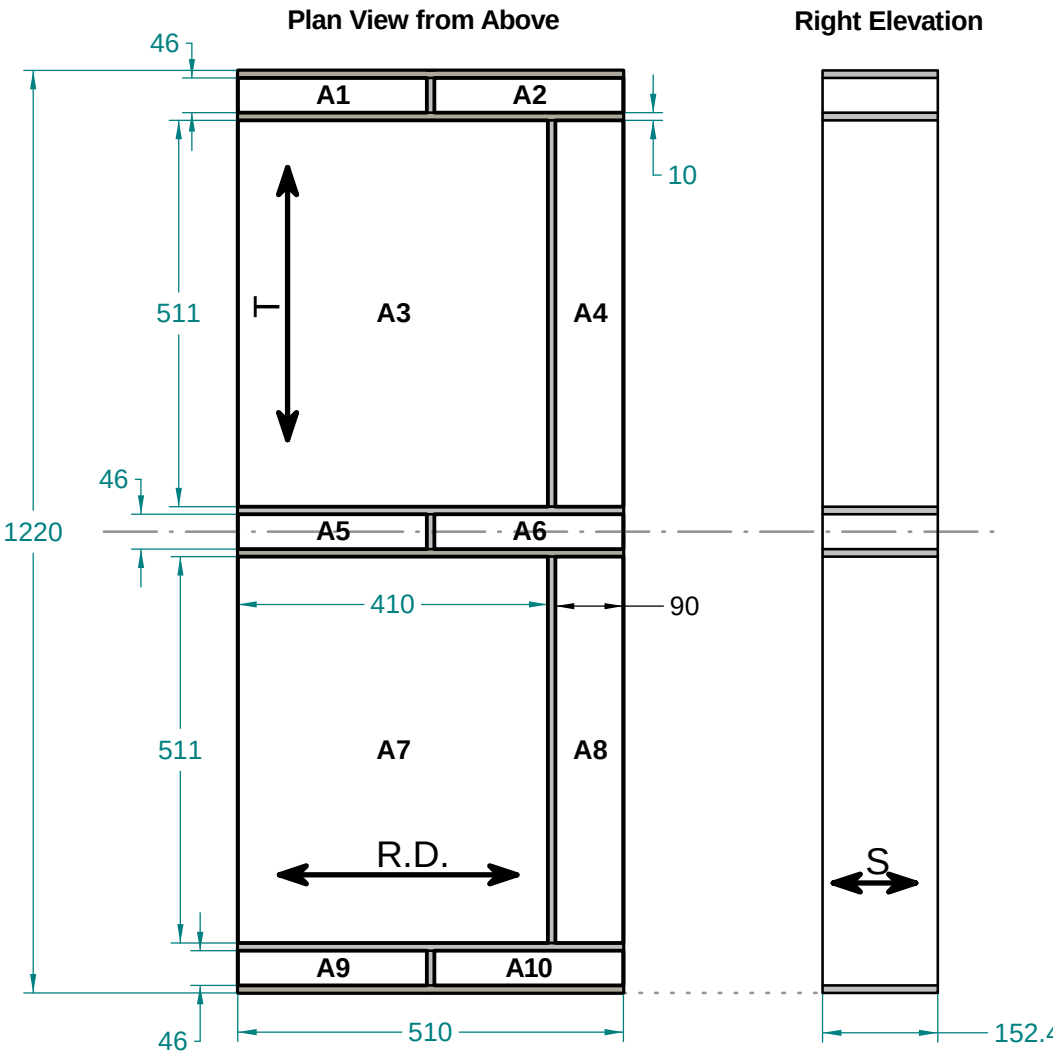

Figure 14: Cut-up diagram of Section A. Dimensions are in millimetres. Cuts between pieces are a maximum of 10 mm thick. R.D. = Rolling Direction (Longitudinal axis), T = Long Transverse and S = Short Transverse. All dimensions are ± 0.1 mm.

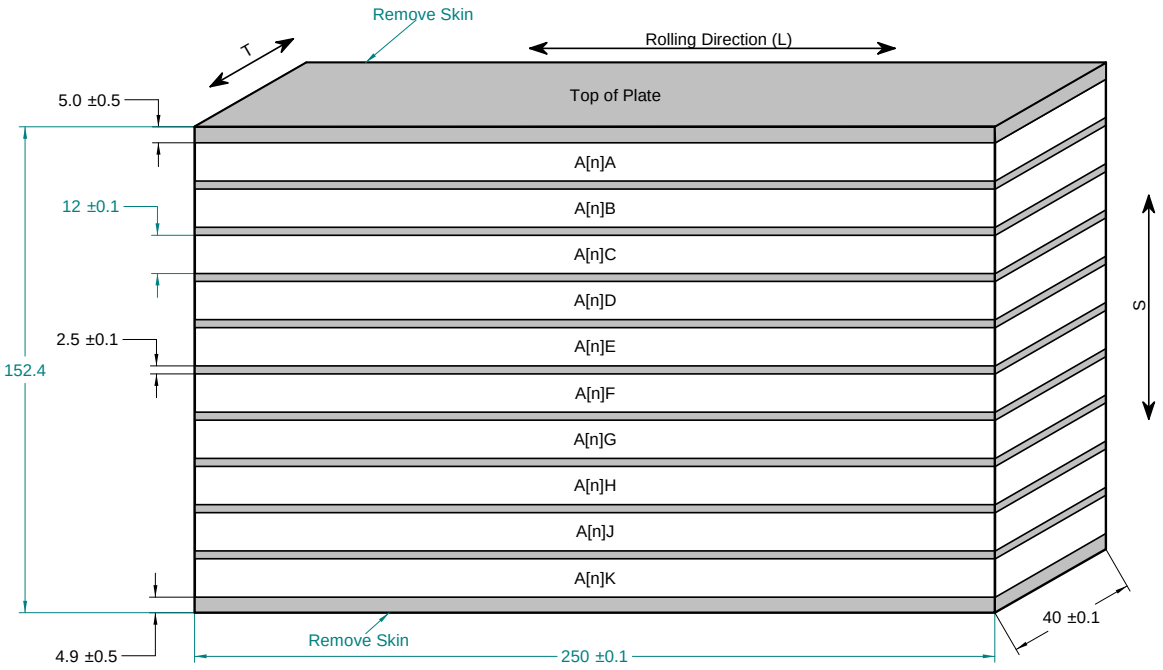

Figure 15: Isometric projection of cut-up of pieces A1, A2, A5, A6, A9 and A10 to create blanks for the high-k_t specimens. Dimensions are in millimetres. Shaded areas are allowances for wire-cutting (2.5 ± 0.1 mm) and removal of the outer layer of the plate (5 and 4.9 mm). Labels A[n]A to A[n]K are identifiers for the specimens. [n] refers to the piece number and is either 1, 2, 5, 6, 9 or 10.

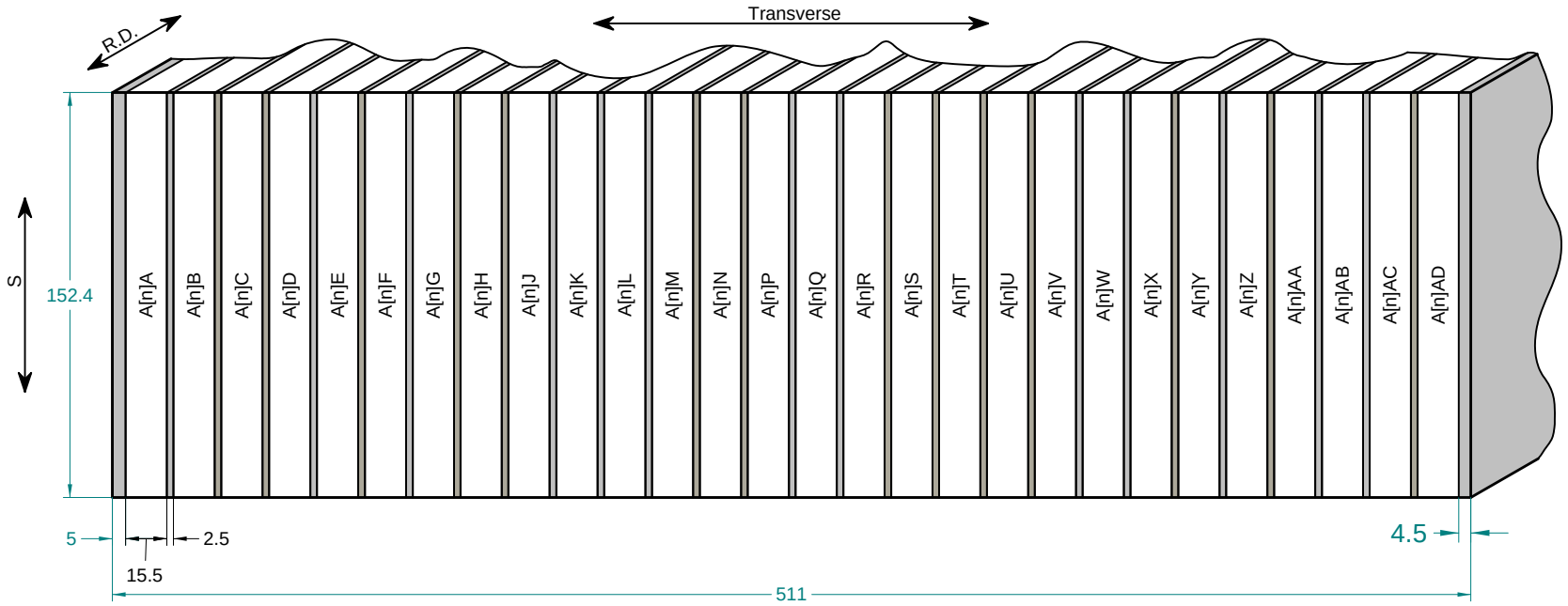

Figure 16: Partial isometric projection of cut-up of pieces A3 and A7. Dimensions are in millimetres. Shaded areas are allowances for wire-cutting (2.5 ± 0.1 mm) and removal of the outer layer of the plate. Labels A[n]A to A[n]Z and A[n]AA to A[n]AD are identifiers for the specimens. [n] refers to the piece number and is either 3 or 7.

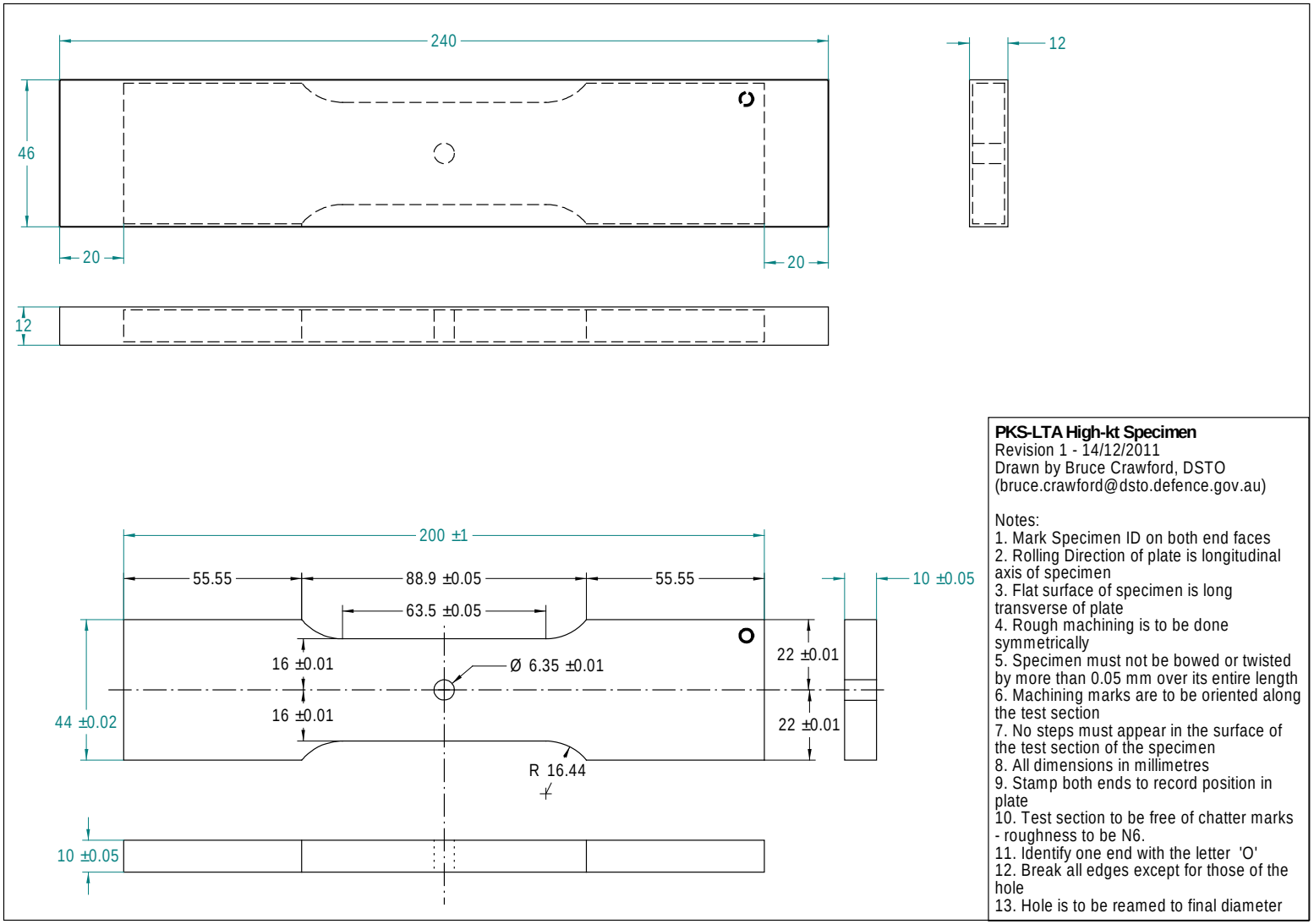

Figure 17: Detailed engineering drawing of the high-k_t fatigue specimens to be machined from material plate MX

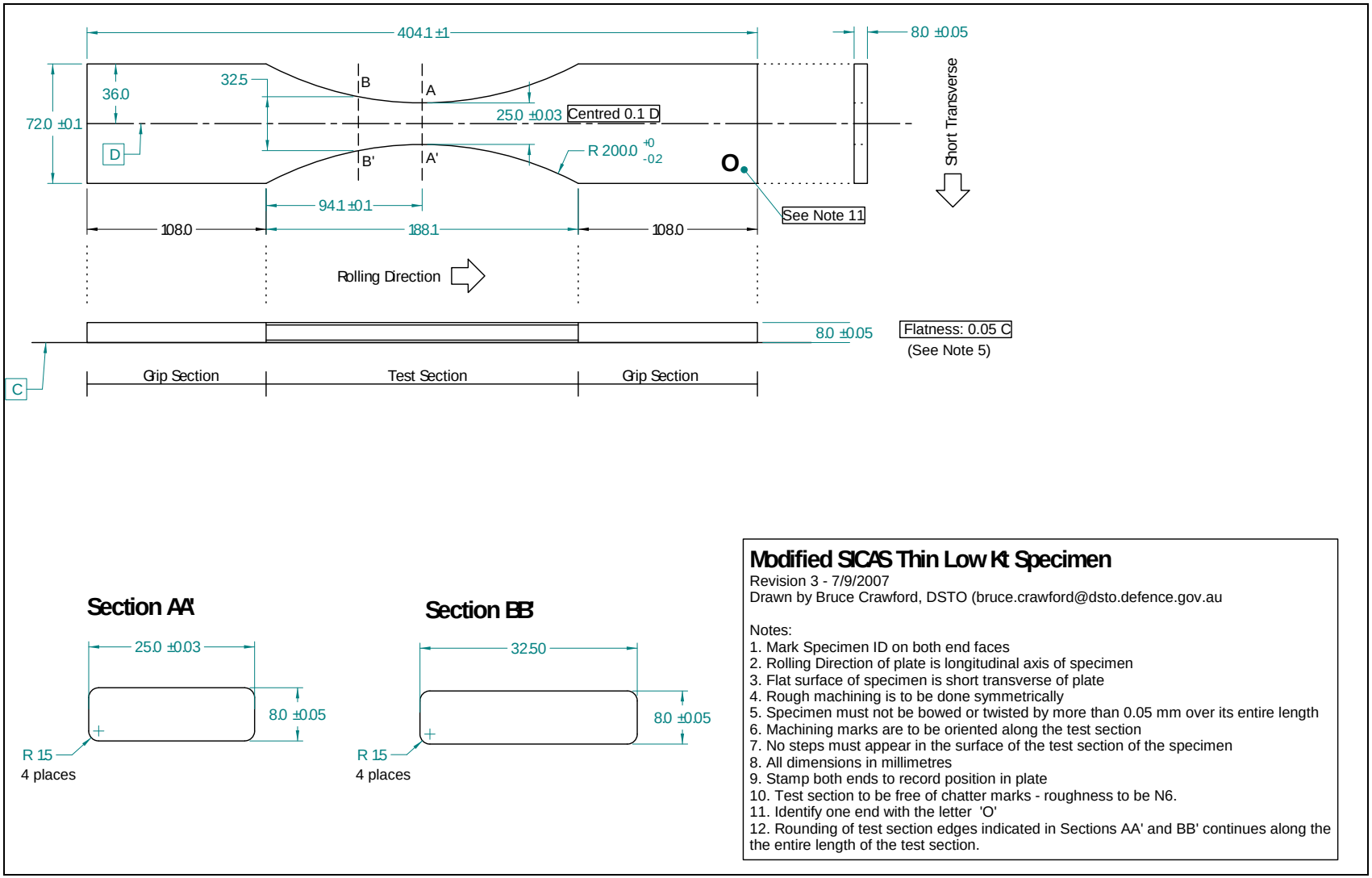

Figure 18: Detailed engineering drawing of the low-k_t fatigue specimens to be machined from material plate MX

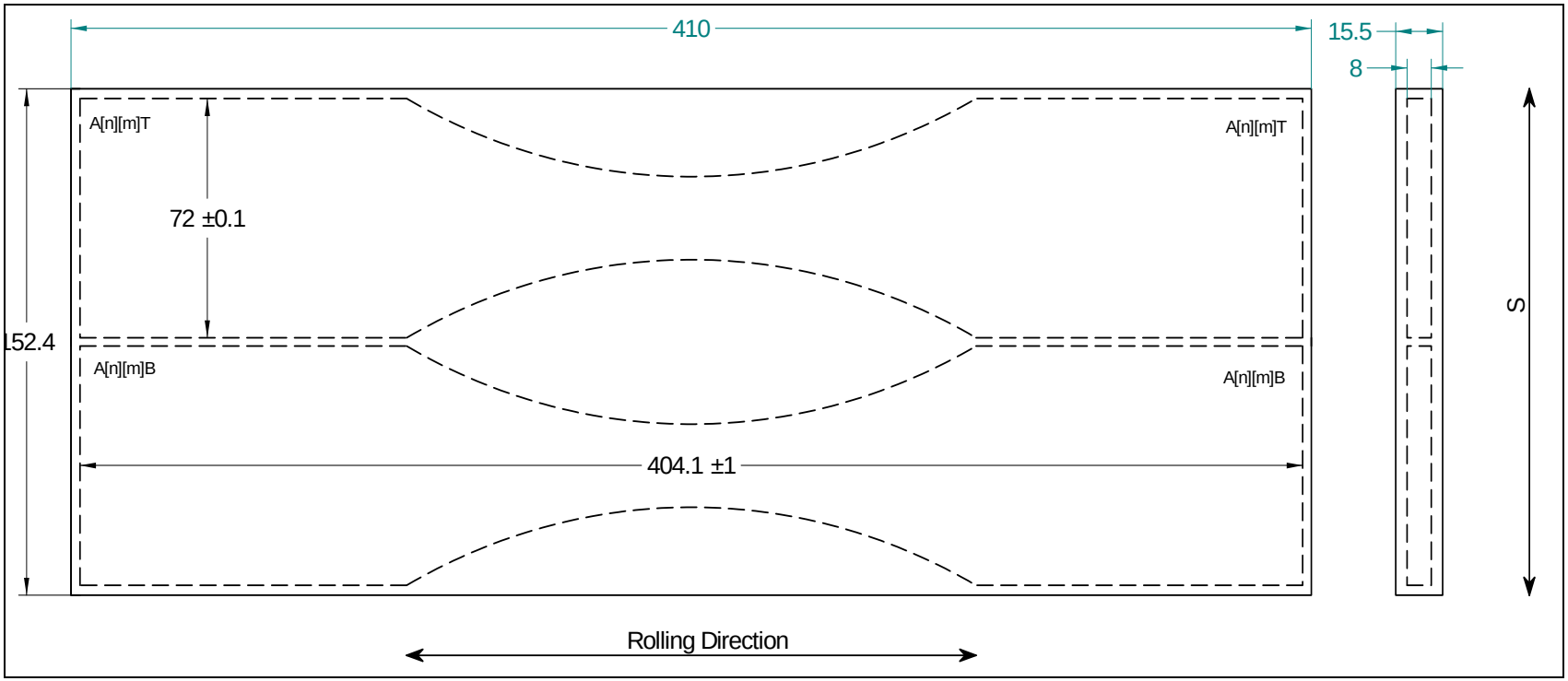

Figure 19: Position of low-k_t specimens in blanks cut from pieces A3 and A7. Two low-k_t specimens will be machined from each blank. The position of these specimens in the blanks are shown by the dashed lines. 'A[n][m]T' and 'A[n][m]B' respectively identify the upper and lower specimens from each blank.

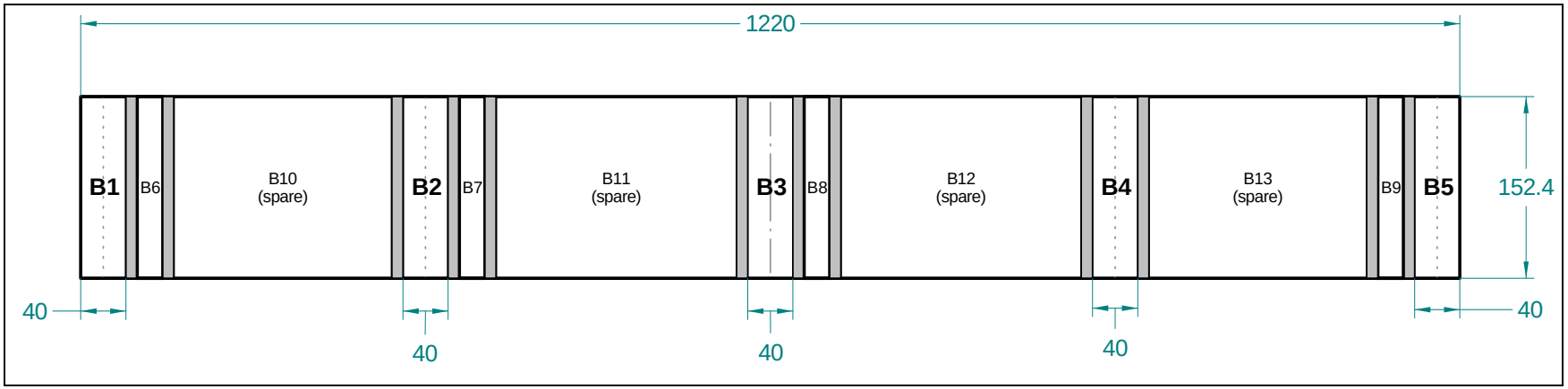

Figure 20: Cut-up of Plate MX Section B showing position and size of Blocks B1 to B13. The shaded areas are cutting allowances which are assumed to be a maximum of 10 mm thick. All dimensions are in millimetres.

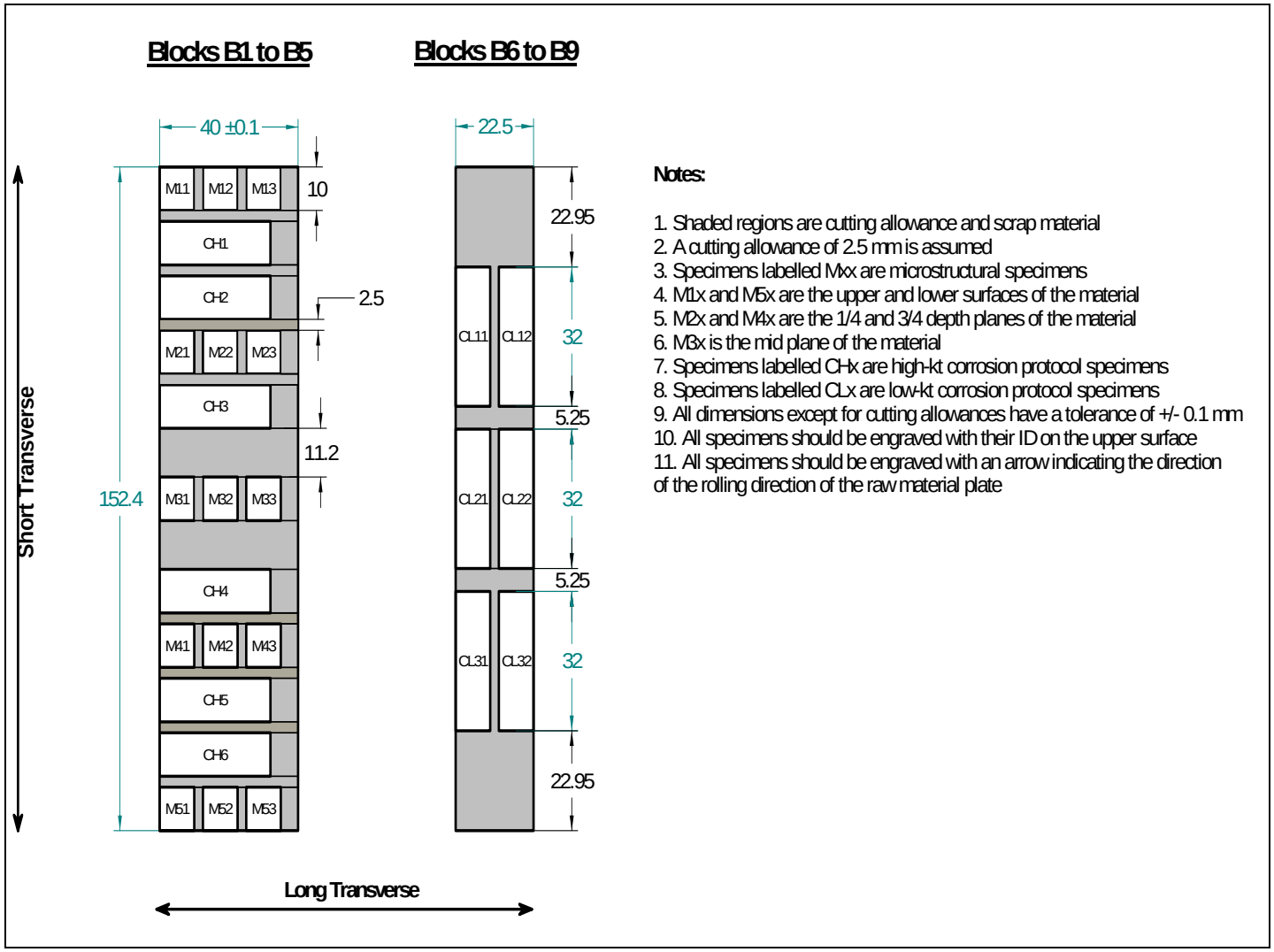

Figure 21: Cut-up diagram of Blocks B1 to B5 and B6 to B9 (right). All dimensions are in millimetres.

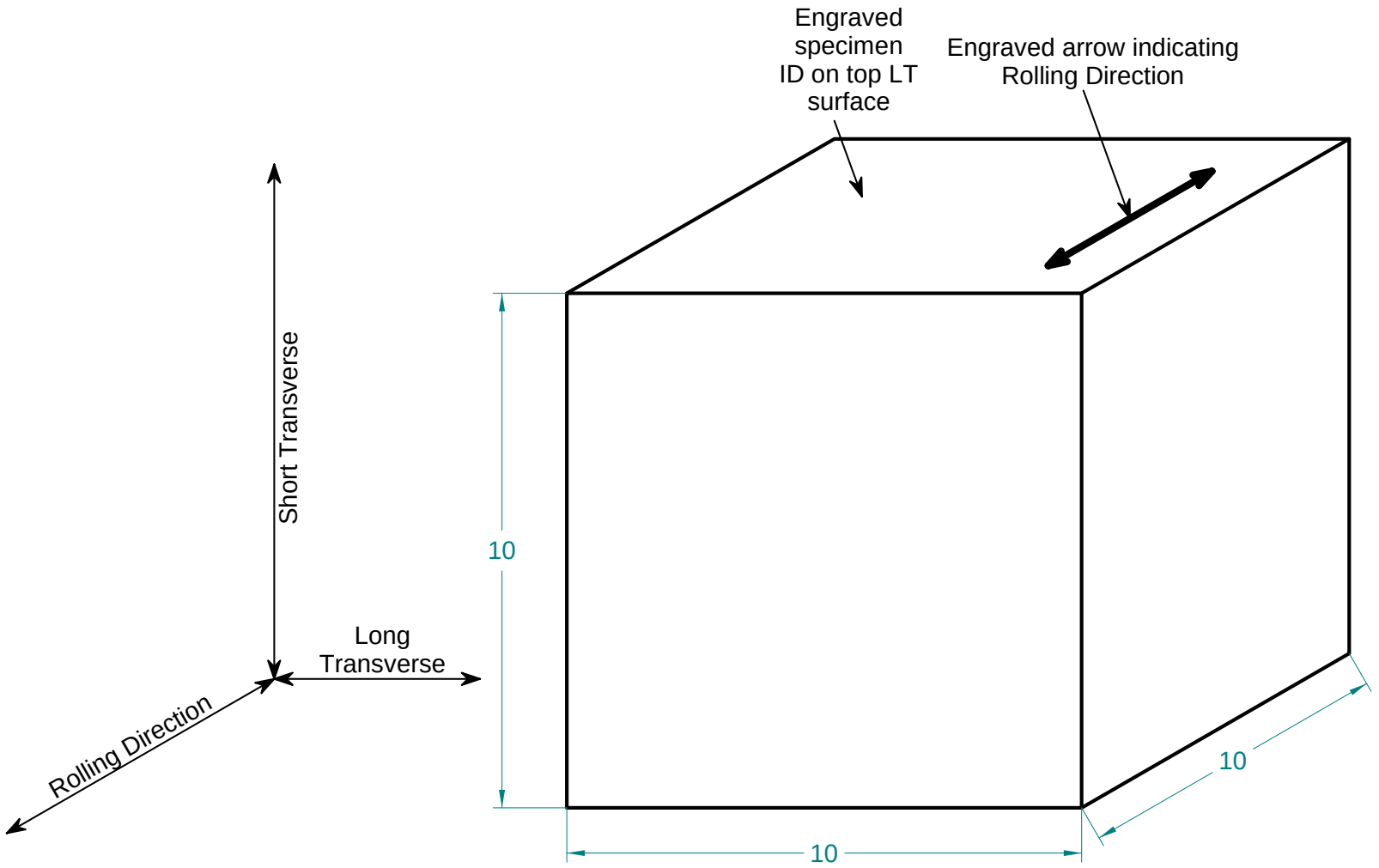

Figure 22: Engineering drawing of the microstructural specimens showing the location of the specimen ID and of the arrow showing the rolling direction of the material. All dimensions are in millimetres. All dimensions are ± 0.1 mm.

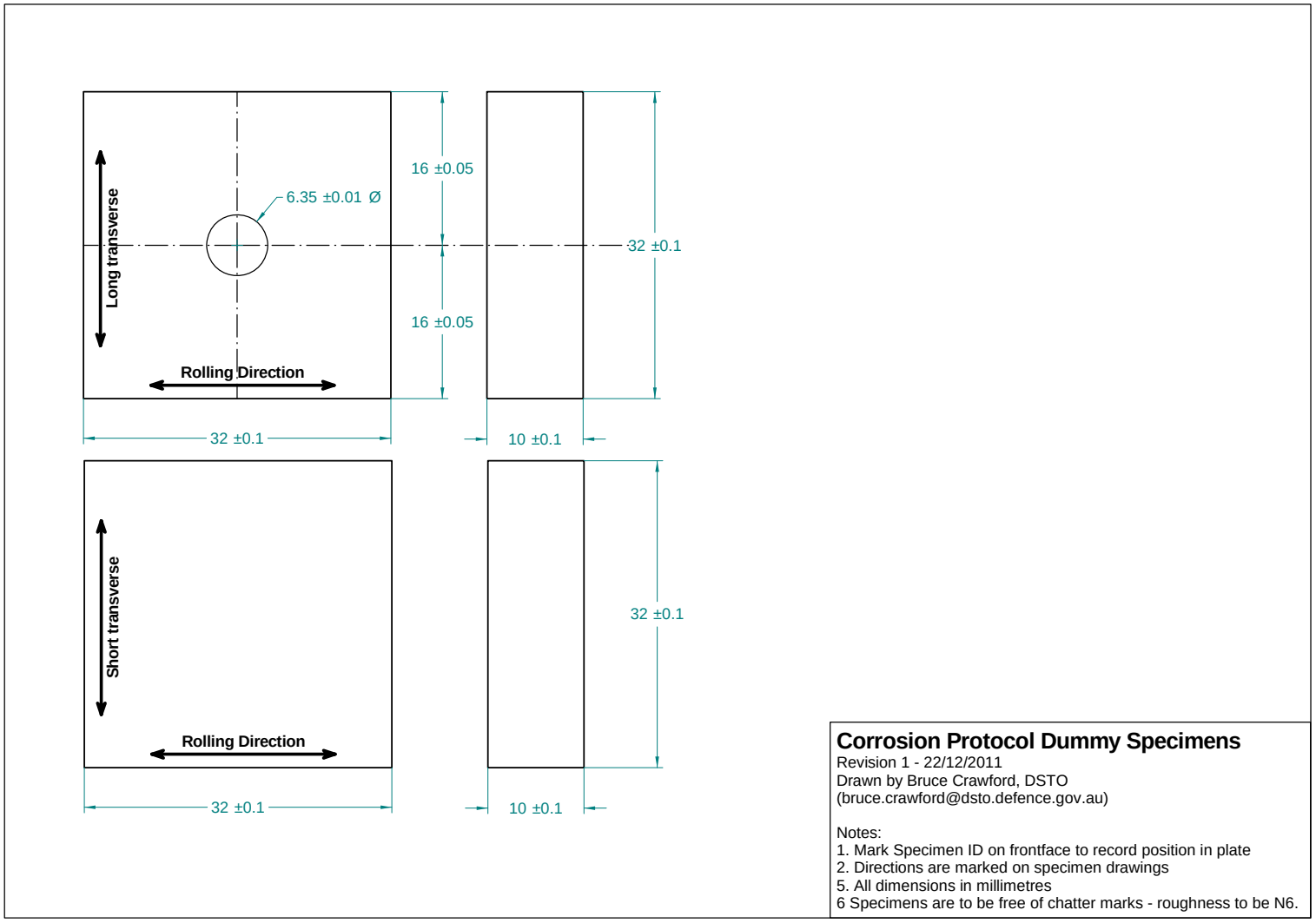

Figure 23: Engineering drawings of the high and low-k_t corrosion protocol dummy specimens to be machined from material plate MX Section B.

DEFENCE SCIENCE AND TECHNOLOGY ORGANISATION
DOCUMENT CONTROL DATA

1. PRIVACY MARKING/CAVEAT (OF DOCUMENT)

2. TITLE

Experimental Plan for the Development of Equivalent Crack Size Distributions and a Monte Carlo Model of Fatigue in Low and High-k_t Specimens of Corroded AA7050-T7451

3. SECURITY CLASSIFICATION (FOR UNCLASSIFIED REPORTS THAT ARE LIMITED RELEASE USE (L) NEXT TO DOCUMENT CLASSIFICATION)

Document	(U)
Title	(U)
Abstract	(U)

4. AUTHOR(S)

Bruce R. Crawford, Timothy J. Harrison, Chris Loader and P. Khan Sharp

5. CORPORATE AUTHOR

DSTO Defence Science and Technology Organisation
506 Lorimer St
Fishermans Bend Victoria 3207 Australia

6a. DSTO NUMBER	6b. AR NUMBER	6c. TYPE OF REPORT	7. DOCUMENT DATE
DSTO-TN-1073	AR-015-242	Technical Report	March 2012

8. FILE NUMBER	9. TASK NUMBER	10. TASK SPONSOR	11. NO. OF PAGES	12. NO. OF REFERENCES
2012/1014211/1	07/282	AVD	42	20

13. DSTO Publications Repository

http://dspace.dsto.defence.gov.au/dspace/

14. RELEASE AUTHORITY

Chief, Air Vehicles Division

15. SECONDARY RELEASE STATEMENT OF THIS DOCUMENT

Approved for public release

OVERSEAS ENQUIRIES OUTSIDE STATED LIMITATIONS SHOULD BE REFERRED THROUGH DOCUMENT EXCHANGE, PO BOX 1500, EDINBURGH, SA 5111

16. DELIBERATE ANNOUNCEMENT

No Limitations

17. CITATION IN OTHER DOCUMENTS Yes

18. DSTO RESEARCH LIBRARY THESAURUS

Aircraft, Structural Integrity, Corrosion, Corrosion Fatigue, Monte Carlo method

19. ABSTRACT

Fatigue life data from low and high-k_t specimen are difficult to compare due to the smaller sampling volume of high-k_t specimens. As a result, equivalent crack size (ECS) distributions developed using low-k_t specimens cannot be used in high-k_t conditions such as near fastener holes. This experimental plan addresses this issue for corroded AA7050-T7451. Fatigue crack growth (FCG) and fatigue life tests will be conducted on low and high-k_t specimens which have been designed to minimise the differences between the specimens other than the different stress field. FCG data and ECS distributions will be developed for both specimens types. A Monte Carlo model will then be used to test if the low-k_t ECS distribution can accurately predict the fatigue lives of the high-k_t specimens. If successful, this will allow low-k_t ECS distributions, which are easier to derive, to be used under high-k_t conditions.